Molecular Communications: Novel Relaying Schemes and Molecular Beamforming

by

Joana Angjo

A Dissertation Submitted to the
Graduate School of Sciences and Engineering
in Partial Fulfillment of the Requirements for
the Degree of

Master of Science

in

Electrical and Electronics Engineering

KOÇ ÜNİVERSİTESİ

June, 2022

Molecular Communications: Novel Relaying Schemes and Molecular Beamforming

Koç University

Graduate School of Sciences and Engineering

This is to certify that I have examined this copy of a master's thesis by

Joana Angjo

and have found that it is complete and satisfactory in all respects,
and that any and all revisions required by the final
examining committee have been made.

Committee Members:

_____

Assoc. Prof. Ertuğrul Başar (Advisor)

_____

Prof. Ali Emre Pusane [Co-Advisor]

_____

Assist. Prof. Murat Kuşcu

Date: _____

In dedication to my dear parents and siblings.

Në përkushtim ndaj prindërve, motrës dhe vëllait të mi të dashur.

ABSTRACT

Molecular Communications: Novel Relaying Schemes and Molecular Beamforming
Joana Angjo
Master of Science in Electrical and Electronics Engineering
June, 2022

The communication in the small scale has received a growing interest in the recent years due to two main reasons. First of all, there is a wide variety of applications for which the traditional communication technologies are not suitable, especially those related to medical treatment and healthcare. Secondly, the communication in the nano/micro scale is feasible due to the advancements in the production of the electronic devices, both in terms of cost and scale constraints. As a prominent approach towards enabling nanonetworking, molecular communications (MC) has been proposed. First and foremost, compared to the conventional EM communication, MC solves the impediment of the size of antennas. Moreover, MC is a bio-compatible solution, which is a key aspect for its proposed usage areas.

There exist numerous MC systems introduced in the literature, among which MC via diffusion (MCvD) is one of the most examined ones, since it is an efficient and practical solution that utilizes the diffusive characteristics of molecules for conveying the information. The signal arriving at the intended node features a heavy-tail shape due to the diffusion dynamics of the molecules, which leads to the MCvD systems being prone to inter-symbol interference (ISI). Alleviating ISI is one of the most investigated issues when it comes to MC. Apart from that, the communication range is another limitation that characterizes MCvD, due to the signal's amplitude rapidly decreasing as the communicating nanomachines get further from each other. In order to address these challenges, novel designs and algorithms in the communication perspective are proposed in the literature.

Chapter 2 of this dissertation summarizes the single-input single-output (SISO) topology of MCvD, providing the foundations in the literature that are very useful in understanding the aforementioned challenges. Moreover, a brief literature review on relaying in MC is provided, laying the groundwork for the motivation behind two

of the contributions of this dissertation.

The first proposed scheme is introduced in Chapter 3. This work is inspired from the fact that most of the relay-based schemes in the literature of MC consider the relay to be positioned in the middle of the two nodes whose communication it facilitates. As this my not always be achievable in practice, an asymmetrical relaying case is considered. If the parameters of the two resulting communication links have the same values, the overall performance of an asymmetrical relaying scheme is prone to error propagation due to unequal error protection for these links. This results from the fact that the quality of the channel belonging to the node closer to the relay is higher compared to the channel of the further one. In order to overcome this, utilization of molecules with different diffusion coefficients is proposed for the uplink (UL) of the relaying system. The best performance in terms of bit error rate (BER) is obtained when the emitting points release different numbers of different types of molecules. Two parameter optimization methods are proposed and the analytical results are verified by computer simulations.

The scheme proposed in Chapter 4 focuses on utilizing a relay for boosting the received signal's strength, which results in an improvement in the BER performance of the communication system. This scheme is referred to as optimal relaying. The proposed system consists of a transmitting point, a receiving node, and a relay somewhere in between them. The relay absorbs a fraction of the released molecules, until some time, and then re-directs it towards the receiver (Rx), which also absorbs from the molecules emitted from the transmitter (Tx) in the meantime. In other words, the overall absorbed molecules at the Rx come from two sources: the Tx and the relay. Overlapping these two components, such that the overall amplitude of the received signal is increased, is the main motivation of this work. In order to achieve this, optimizing the time until when the relay will be absorbing is proposed by means of maximizing a function called the signal to interference difference (SID). The system is modelled analytically as well. The BER results after optimization are compared with the BER performance of the traditional SISO system, and an improvement is shown to be attained with the incorporation of the optimal relay.

The last contribution of the thesis focuses on cooperative sensing in MCvD networks. Particularly, a novel paradigm is presented, which is motivated by specific scenarios where MC can find application, such as sugar level stabilization of patients with diabetes. Inspired by the concept of beamforming in radio frequency (RF) communications, molecular beamforming is presented in Chapter 5. The proposed

technique can find application in systems where the actuation of nanomachines is targeted. The typical proposed network consists of several sensors (Txs) that emit molecules with the purpose of activating one actuator (Rx) at a time, whose on or off state depends on the overall received signal. However, the sensors are prone to errors, thus they may wrongly emit/not emit. For this reason, the main motivation behind this idea is that when the number of sensors increases, the actuation error rate decreases. In order to achieve this, several design techniques are proposed, such that the overall received signal is composed of delayed versions of the components arriving from different sensors. The verification of the proposed method is achieved by the analytical derivation of the actuation error probability for several scenarios. Firstly, the system where sensors are forming a uniform linear array (ULA) is considered for presenting the scheme with less complexity. Afterwards, a more realistic scenario is considered, where the locations of the sensors are random. As for the computation of the actuation error rate, three different scenarios are presented, depending on the error source and how the actuation decision is made. The analytical results are validated with the ones obtained from computer simulations. The results reveal very interesting insights about the potential of molecular beamforming for actuation accuracy in MC networks.

Finally, Chapter 6 concludes the dissertation by summarizing the main outcomes obtained from the aforementioned works. Additionally, several future research directions are provided.

ÖZETÇE

Yüksek Lisans Tez Başlığı
Joana Angjo
Elektrik ve Elektronik Mühendisliği, Yüksek Lisans
Haziran, 2022

Küçük ölçekte iletişim, iki ana nedenden dolayı son yıllarda artan bir ilgi görmüştür. Her şeyden önce, geleneksel iletişim teknolojilerinin uygun olmadığı, özellikle tıbbi tedavi ve sağlıkla ilgili çok çeşitli uygulamalar vardır. İkincisi, elektronik cihazların üretimindeki gelişmeler nedeniyle nano/mikro ölçekte iletişim, hem maliyet hem de ölçek kısıtlamaları açısından uygulanabilir. Nano ağ oluşturmayı etkinleştirmeye yönelik belirgin bir yaklaşım olarak moleküler iletişim (molecular communications, MC) önerilmiştir. Her şeyden önce, geleneksel EM iletişimiyle karşılaştırıldığında, MC, anten boyutundaki engeli çözmektedir. Ayrıca MC, önerilen kullanım alanları için önemli bir özellik olan biyo-uyumlu bir çözümdür.

Literatürde tanıtılan çok sayıda MC sistemi vardır; bunların arasında, bilgiyi iletmek için moleküllerin yayılma özelliklerini kullanan verimli ve pratik bir çözüm olduğu için, difüzyon yoluyla MC (MC via diffusion, MCvD) en çok incelenenlerden biridir. Amaçlanan düğüme ulaşan sinyal, moleküllerin difüzyon dinamikleri nedeniyle ağır bir kuyruk şekline sahiptir, bu da MCvD sistemlerinin semboller arası girişime (inter-symbol interference, ISI) eğilimli olmasına yol açar. ISI'yı hafifletmek, MC söz konusu olduğunda en çok araştırılan konulardan biridir. Bunun dışında, iletişim aralığı, iletişim kuran nanomakineler birbirinden uzaklaştıkça sinyalin genliğinin hızla azalması nedeniyle MCvD'yi karakterize eden başka bir sınırlamadır. Bu zorlukların üstesinden gelmek için literatürde iletişim perspektifinde yeni tasarımlar ve algoritmalar önerilmiştir.

Bölüm 2, MCvD'nin tek girişli tek çıkışlı (single-input single-output, SISO) topolojisini özetleyerek, yukarıda bahsedilen zorlukları anlamada çok yararlı olan literatürdeki temelleri sağlar. Ayrıca, bu tezin iki katkısının ardındaki motivasyon için zemin hazırlayan MC'de aktarma üzerine kısa bir literatür taraması sağlanmıştır.

Önerilen ilk şema Bölüm 3'te tanıtılmıştır. Bu çalışma, MC literatüründeki röle tabanlı şemaların çoğunun, rölenin iletişimini kolaylaştırdığı iki düğümün or-

tasında konumlandığını düşünmesinden esinlenmiştir. Bu, pratikte her zaman elde edilemediğinden, asimetrik bir aktarma durumu düşünülür. Ortaya çıkan iki iletişim bağlantısının parametreleri aynı değerlere sahipse, asimetrik bir geçiş şemasının genel performansı, bu bağlantılar için eşit olmayan hata koruması nedeniyle hata yayılımına eğilimlidir. Bu, röleye yakın olan düğüme ait kanalın kalitesinin, röleye yakın olanın kanalına göre daha yüksek olmasından kaynaklanmaktadır. Bunun üstesinden gelmek için, geçiş sisteminin yukarı yönlü aktarım'i (UL) için farklı difüzyon katsayılarına sahip moleküllerin kullanılması önerilmiştir. Bit hata oranı (bit error rate, BER) açısından en iyi performans, yayan noktalar farklı sayıda farklı molekül türü serbest bıraktığında elde edilir. İki parametreli optimizasyon yöntemi önerilmiş ve analitik sonuçlar bilgisayar simülasyonları ile doğrulanmıştır.

Bölüm 4'te önerilen şema, alınan sinyalin gücünü artırmak için bir röle kullanmaya odaklanmaktadır, bu da iletişim sisteminin BER performansında bir gelişme ile sonuçlanmaktadır. Bu şema, optimal geçiş olarak adlandırılmaktadır. Önerilen sistem, bir verici nokta, bir alıcı düğüm ve bunların arasında bir yerde bir röleden oluşur. Röle, bir süreye kadar salınan moleküllerin bir kısmını emer ve daha sonra onu, bu arada vericiden (transmitter, Tx) yayılan moleküllerden de emen alıcıya (receiver, Rx) doğru yönlendirir. Başka bir deyişle, Rx'de toplam absorbe edilen moleküller iki kaynaktan gelir: Tx ve röle. Alınan sinyalin genel genliği artırılacak şekilde bu iki bileşenin örtüşmesi bu çalışmanın ana motivasyonudur. Bunu başarmak için, sinyal-girişim farkı (signal to interference difference, SID) olarak adlandırılan bir fonksiyonun maksimize edilmesi yoluyla rölenin soğurulacağı zamana kadar olan sürenin optimize edilmesi önerilmiştir. Sistem analitik olarak da modellenmiştir. Optimizasyondan sonraki BER sonuçları, geleneksel SISO sisteminin BER performansı ile karşılaştırılır ve optimal rölenin dahil edilmesiyle bir iyileştirme elde edildiği gösterilmektedir.

Tezin son katkısı, MCvD ağlarında işbirlikli algılamaya odaklanmaktır. Özellikle, diyabetli hastaların şeker seviyesi stabilizasyonu gibi MC'nin uygulama bulabileceği belirli senaryolar tarafından motive edilen yeni bir paradigma sunulmaktadır. Radyo frekansı (radio frequency, RF) iletişiminde huzme oluşturma kavramından ilham alan moleküler huzme oluşturma, Bölüm 5'te sunulmaktadır. Önerilen teknik, nanomakinelerin harekete geçirilmesinin hedeflendiği sistemlerde uygulama bulabilir. Önerilen tipik ağ, açık veya kapalı durumu alınan genel sinyale bağlı olan bir seferde bir aktüatörü (Rx) etkinleştirmek amacıyla moleküller yayan birkaç sensörden (Txs) oluşur. Bununla birlikte, sensörler hataya eğilimlidir, bu nedenle yanlış bir şekilde

yayabilir/yaymayabilirler. Bu nedenle, bu fikrin arkasındaki ana motivasyon, sensör sayısı arttıkça çalıştırma hata oranının azalmasıdır. Bunu başarmak için, alınan genel sinyalin farklı sensörlerden gelen bileşenlerin gecikmeli versiyonlarından oluştuğu şekilde çeşitli tasarım teknikleri önerilmiştir. Önerilen yöntemin doğrulanması, birkaç senaryo için çalıştırma hatası olasılığının analitik olarak türetilmesiyle sağlanır. İlk olarak, şemayı daha az karmaşıklıkla sunmak için sensörlerin düzgün bir doğrusal dizi (uniform linear array, ULA) oluşturduğu sistem düşünülmüştür. Ardından sensörlerin konumlarının rastgele olduğu daha gerçekçi bir senaryo düşünülmektedir. Çalış- tırma hata oranının hesaplanmasına gelince, hata kaynağına ve çalıştırma kararının nasıl verildiğine bağlı olarak üç farklı senaryo sunulmuştur. Analitik sonuçlar bilgisayar simülasyonlarından elde edilenlerle doğrulanmıştır. Sonuçlar, MC ağlarında harekete geçirme doğruluğu için moleküler hüzme şekillendirme potansiyeli hakkında çok ilginç bilgiler ortaya koyulmaktadır.

Son olarak, Bölüm 6, yukarıda bahsedilen çalışmalardan elde edilen ana sonuçları özetleyerek tezi sonlandırmaktadır. Ek olarak, gelecekteki birkaç araştırma yönü sunulmuştur.

ACKNOWLEDGMENTS

I would like to express my heartfelt acknowledgement to my dear advisor, Assoc. Prof. Ertuğrul Başar for his continuous assistance and support during my studies. From when I completed my internship near the CoreLab team in 2019, he has been a role model to me. He has continuously provided me with very valuable feedback and a very encouraging research environment. It has been such an honour for me to work under his guidance.

Secondly, I would like to express my deepest gratitude to my dear co-advisor, Prof. Ali Emre Pusane, for his consistent assistance of my studies. His patience, dedication and enthusiasm have been really inspiring and have helped me to improve both academically and as a person. It has been a huge privilege for me to work with him.

Many thanks to Prof. Tuna Tuğcu and Asst. Prof. H. Birkan Yılmaz for their constructive suggestions and advice, as well as for all the valuable discussions that we have had during my studies.

I am extremely grateful for my friends, who have been by my side throughout my ups and downs. A special thanks goes to Serhan Kaya and Fregis Sala, my go-tos, without whom I would have never made it!

I would like to express my profound appreciation to my mother Anila, my father Kelment and my siblings, Sara and Anxhelin for their never-ending encouragement, trust and love. You have always believed in me and I hope I can make you half as proud as you make me everyday. I am, because you are.

Lastly, I would like to express my acknowledgment to Technical Research Council of Turkey (TUBITAK) for funding my M.Sc studies as part of the project under Grant 119E190.

TABLE OF CONTENTS

LIST OF TABLES

LIST OF FIGURES

ABBREVIATIONS

3-D	Three-Dimensional
AF	Amplify-and-Forward
BER	Bit Error Rate
BMoSK	Binary Molecule Shift Keying
CDF	Cumulative Distribution Function
CFAM	Cumulative Fraction of Absorbed Molecules
CNN	Convolutional Neural Networks
CSK	Concentration Shift Keying
DF	Decode-and-Forward
DFE	Decision Feedback Equalizer
DL	Downlink
D-MoSK	Depleted Molecule Shift Keying
EM	Electromagnetic
EF	Estimate-and-Forward
IEEE	Institute of Electrical and Electronics Engineering
ILI	Inter-Link Interference
IM	Index-Modulation
ISI	Inter-Symbol Interference
LoS	Line-of-Sight
MAP	Maximum a Posteriori
MC	Molecular Communication
MCvD	Molecular Communication via Diffusion
MEP	Minimum Error Probability
ML	Machine Learning
MLD	Maximum Likelihood Detection

MIMO	Multiple-Input Multiple-Output
MMSE	Minimum Mean-Square Error
MoSK	Molecule Shift Keying
MSM	Molecule Spatial Modulation
MSSK	Molecule Space Shift Keying
NLoS	Non-Line-of-Sight
OOK	On-Off Keying
PDF	Probability Density Function
Rx	Receiver
QMSSK	Quadrature Molecule Space Shift Keying
RF	Radio Frequency
RIS	Reconfigurable Intelligent Surfaces
RTSK	Release Time Shift Keying
SID	Signal to Interference Difference
SIMO	Single-Input Multiple-Output
SISO	Single-Input Single-Output
TNB	Transactions on NanoBioscience
Tx	Transmitter
UL	Uplink
ULA	Uniform Linear Array
ZF	Zero-Forcing

Chapter 1

INTRODUCTION

The ability to convey information over a distance has revolutionized the human life over the course of time. As a result of the continuous evolution in the area of communication technologies, cutting edge systems have been developed, traditionally utilizing electromagnetic (EM) communication. Nonetheless, there are applications for which EM communication is not convenient or feasible. For instance, several complex environments with obstacles are studied in [Guo et al., 2015], showing that for such scenarios, EM communication may be disadvantageous. Its impracticability also arises for small scale communication systems. As a result, some studies have focused on optical communications for the small scale [Alomainy et al., 2019]. However, optical communications is not feasible as well, due to the requirement of guided medium and the limitations characterizing it. As a result, novel communication paradigms necessitate for when the conventional ones are not appropriate.

Molecular communications (MC) is an emerging communication paradigm inspired by biological systems, which has established the idea of structured communication in which the molecule-based signals convey information between nanomachines [Hiyama et al., 2006]. There are several distinctions between MC and EM communications, several of which are summarized in Table 1.1 There is actually a variety of MC examples in the real world, whose principles are followed in the MC networks. The basis of cell communication through different kinds of signalling molecules is explained by the authors of [Alberts et al., 2003]. Basically, a signalling cell secretes molecules, which are captured by the targeting cell, usually through the process of binding into its receptors with the purpose of initiating a specific kind of

Table 1.1: The differences between MC and EM communications.

Communication Type	MC	EM
Signal Type	Chemical	Electrical
Communication Carrier	Molecules	EM waves
Speed	Very low	Very high
Communication Range	nm/μm	m/km
Media	Usually aqueous	Air, cables, optical fiber etc.
Energy efficiency	Higher	Lower

response by this target cell. Other examples in the nature include hormonal communication (long range MC), bacterial conjugation (medium range MC), molecular motors (short range MC), etc. [Akyildiz et al., 2015]. These examples are illustrated in Figure 1.1, where (a) represents Ca 2+ communication (exchange of calcium ion between two cells), (b) molecular motors, (c) bacteria conjugation-chemotaxis, and (d) hormonal communication.

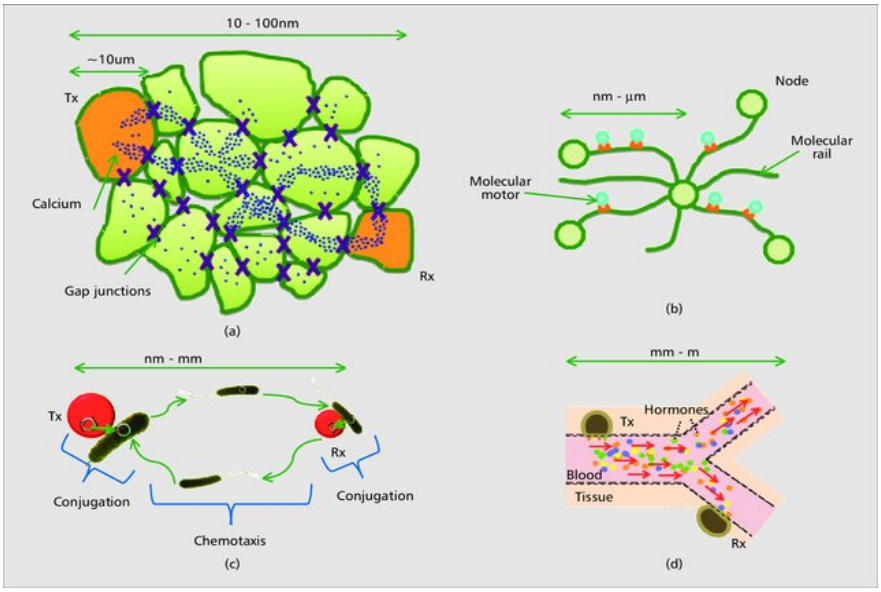

Figure 1.1: Examples of MC in nature [Akyildiz et al., 2015]

.

The paradigm of MC is based on transmitting the information using molecules that diffuse through a fluid environment from the source to the destination. MC has received great attention in recent years in regard to numerous small scale applications, for which EM communication is impractical due to the constraints that characterize these applications [Akyildiz et al., 2008]. One such constraint is the requirement of the antennas' sizes in the nano scale [Galal and Hesselbach, 2018]. Most of the applications in which MC offers promising results are related to medical treatments and human health. MC offers characteristics such as biocompatibility and lowest level of invasion, which make it preferable for health-related applications [Felicetti et al., 2016]. Nano-sensors can be implemented for identifying and even preventing diseases, such as cardiovascular and tumorous disorders. They can be used to find and fight against pathogens, mimicking and carrying out similar functions of immune systems. Additionally, they can reach critical and sensitive locations of the human body, for which traditional solutions fail to do so [Cevallos et al., 2019]. Furthermore, MC provides numerous means for the implementation of drug delivery systems [Chahibi, 2017]. Some studies have also concentrated on beyond free-space applications, such as pipe, knife edge and mesh channels and the presented results show that MC may be more favorable compared to EM communications [Guo et al., 2015]. Apart from these, other applications of MC include also industrial settings, such as food safety and quality monitoring, as discussed in [Fonseca et al., 2007]. The application of nanotechnology in these sectors is promising in terms of rapid response of the nanonetworks, lower overall expenses, and size reduction of the hardware. Furthermore, MC may be advantageous for air pollution control, as discussed in [Han et al., 2008]. Given the aforementioned reasons about its potential, the literature on MC is extensive, consisting of both the analytical foundations of it and practical, real-time applications.

There exist several methods in the literature for enabling MC, each of them characterized by different features. For example, the nanomachines' positions may be fixed or they may be mobile [Varshney et al., 2018a], which is in fact an application-specific characteristic. Moreover, the transmission of the information may solely base on the diffusion of the molecules, or the environment may be characterized by some

drift velocity which affects the propagation of the carriers [Kadloor et al., 2012]. Among several methods proposed in the literature, MC via diffusion (MCvD) is known for being a simple and energy-efficient solution, as the diffusive properties of molecules are utilized for their mobility [Pierobon and Akyildiz, 2010]. Consequently, MCvD is amongst the most preferred and practical methods for MC. In MCvD systems, the information is typically encoded in the characteristics of molecules such as the released amount of molecules [Mahfuz et al., 2010], their types [Gursoy et al., 2019b], release or arrival time [Murin et al., 2017], or other properties. Consequently, there exist different modulation techniques, including on-off keying (OOK) [Kuran et al., 2020], concentration shift keying (CSK) [Shi and Yang, 2017], molecular shift keying (MoSK) [Tepekule et al., 2015a], release time shift keying (RTSK) [Murin et al., 2017] etc.. OOK is the simplest version of CSK modulation, where the transmitter (Tx) emits molecules for bit-1 and stays silent (does not emit) for bit-0. On the other hand, different levels of molecule concentrations for different symbols are used in CSK modulation technique. As for the MoSK modulation technique, different types of molecules are used for the transmission of different symbols. The simplest form of MoSK is binary MoSK (BMoSK), where only two molecule types are used for the transmission of bit-1 and bit-0. A thorough survey of different architectures for the MC network components, including modulation, coding and detection techniques is given in [Kuscu et al., 2019], summarizing the existing literature on MC and pointing out the main challenges faced by it and potential solutions towards them. A rough illustration of a MCvD system consisting on a transmitting and a receiving nanomachine is shown in Figure 1.2. As it can be seen, the molecules propagate in random directions, assuming a boundless environment.

Due to the randomness that characterizes MCvD systems, the signal arriving at the Rx side is classified as a heavy-tailed one, which leads to the systems being prone to inter-symbol interference (ISI) [Tepekule et al., 2015b]. This heavy tail nature of the received signal is caused by the molecules received during the following symbol times after the intended one [Heren et al., 2015]. The alleviation of ISI is directly related to the performance of communication systems, as it deteriorates the

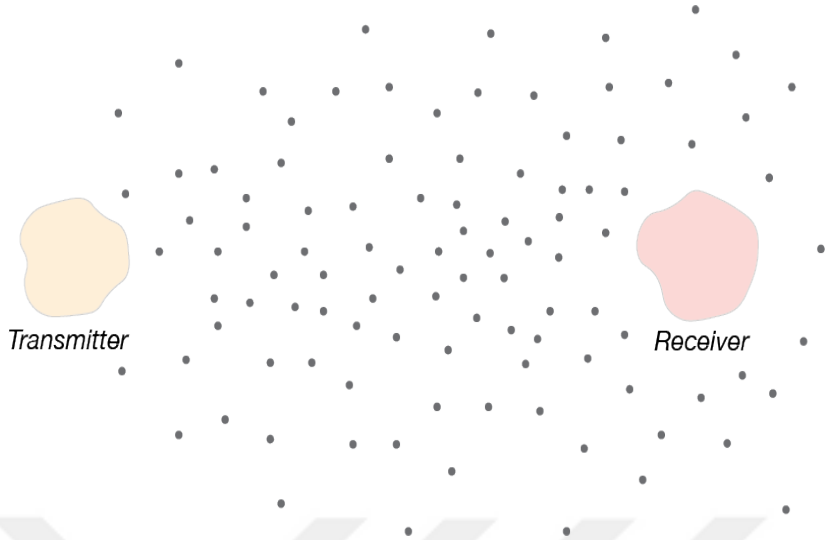

Figure 1.2: An illustration of an MC system consisting of one Tx and one receiver (Rx).

communication reliability and robustness of the MC systems. Many enhancements and modifications towards ISI mitigation are proposed in the literature, such as in [Tepekule et al., 2015a, Koo et al., 2016, Yilmaz and Chae, 2014b, Kislal et al., 2020, Gursoy et al., 2019b]. These solutions include using more than one type of molecules for encoding the signal, novel modulation techniques and/or algorithms that soothe the ISI effect. For example, MoSK modulation is one of the alternatives used for the mitigation of ISI. The authors of [Kilinc and Akan, 2013] propose four different Rx designs that aim to decode and recover the information distorted by ISI and noise. The proposed methods include sequence detection by means of maximum a posteriori (MAP) and maximum likelihood detection (MLD) criteria, such that the observation of the received sequence is used to determine the transmitted sequence by using these criteria to maximize the joint-probability between the transmitted and received sequences. The other techniques include equalization at the Rx, by using minimum mean-square error (MMSE) criterion and decision-feedback equalizer (DFE). Lastly, the authors propose a channel estimator at the Rx. These methods show improvements in term of the reduction of the interference.

The multiple-input multiple-output (MIMO) setting is introduced to MCvD sys-

tems as well. In this case, the diffusive characteristic of the molecules causes inter-link interference (ILI), which is another source of error for the MCvD systems, caused as a result of molecules received by non-intended antennas. The authors of [Gursoy et al., 2019a] propose a novel modulation scheme for the purpose of ILI mitigation. Zero-forcing (ZF) detection is discussed in [Wu et al., 2020] for the cases when ILI is large. Another study is presented in [Gursoy et al., 2019b], where the authors propose molecular index-modulation (IM), using the transmit antenna indices for encoding. In this work, novel modulation techniques are proposed, specifically, molecular space shift keying (MSSK), quadrature MSSK (QMSSK) and molecular spatial modulation (MSM) in order to combat ISI and ILI. QMSSK is shown to alleviate the ISI effect, whereas MSM is proposed for combating ILI more effectively. Molecular IM using convolutional neural networks (CNN) is proposed in [Kara et al., 2021], where the interference effects in a MIMO system are alleviated by the potential of machine learning (ML) based algorithms in recognizing interference patterns in the received signals.

Apart from these challenges, increasing the distance between the Tx and Rx leads to a higher probability of decoding error, thus a limited communication range characterizes MCvD systems. As a result, there are studies in the literature focusing on enabling reliability of these systems while the distance between the nanomachines is increasing. As an example, bounded channels are proposed in the literature as appropriate solutions for long range MC [Giné and Akyildiz, 2009]. Such bounded channels may be modelled as different shapes, such as spherical, rectangular or cylindrical. Relaying in MCvD systems has been also proposed as one of the prominent solutions to the restricted range issue [Einolghozati et al., 2013]. The principle of relaying is facilitatating the communication between two different nanomachines with the help of a third one, through different approaches.

As the focus on MC increases, so does the necessity for the enhancement of these systems, paving the way for novel designs and algorithms that can ensure reliability and robustness in the communication perspective of nanoscale technologies.

1.1 Contributions

The main goal of this dissertation is to explore the existing MC literature and the main challenges faced by this promising paradigm for the communication in small scale. A detailed literature review is provided, and two novel schemes that aim to improve the overall communication performance of MC systems are proposed. Apart from that, this thesis attempts to lay the groundwork towards molecular beamforming through the proposal of a novel outline that can be used for MC networks that target sensor-actuation applications.

Firstly, the limitation of MC systems to short communication ranges is investigated in this thesis. A novel scheme focused on asymmetrical relaying is proposed, inspired from the fact that most of the existing schemes in the literature consider symmetrical setups (the relay is placed in the middle of the communicating nodes), which may not be feasible in practical applications. The proposed system consists of two Txs and a relay placed in between them. The study considers two asymmetrical communication links, for which two different approaches are proposed such that an overall satisfactory performance is achieved in spite of the asymmetry in between. Two different parameter optimization problems are proposed, both focusing on transmitting molecules with different diffusion characteristics from the Txs, such that an equal error protection is achieved for both links, thus also leading to communication fairness for the two Txs. Thus, the proposed solution targets reducing error propagation, and as a result, increasing reliability. The proposed solution focuses on improving the link with the worst quality, without deteriorating the quality of the other link. The performance analysis and evaluation of the proposed solutions are given by providing the channel coefficients of the two communication links, as well as bit error rate (BER) performance curves. It is shown that fairness and equal error protection can be achieved by a good design effort for such an asymmetrical relaying system, following the proposed optimization techniques.

The next proposed scheme is focused on enhancing the received signal shape for a Tx-Rx pair by introducing a relay in between them that "facilitates" the transmission. The main motivation behind this scheme, named as optimal relaying,

is the fact that signal's strength gets rapidly weaker as the distance between the nanomachines increases. For this reason, the relay in between them will receive and collect a fraction of the emitted molecules for some time interval after the emission, and then re-transmit them towards the Rx. As expected, this boosts the signal's strength at the Rx side and the overall performance of the system. Since the Rx will be receiving molecules directly from the Tx as well, an optimization is required for finding the best time interval for which the relay collects molecules from the Tx. The optimization of this parameter, which is referred to as the delay time, τ, aims to minimize the BER performance of the system. In this study, an analytical model for this system is provided, from which τ optimization is derived. This analytical model is compared with the simulation results and as for the performance evaluation, the optimal relaying is compared with the conventional MCvD system, showing a promising improvement in overall system's performance.

The final contribution of this dissertation is the proposal of molecular beamforming for MC networks targetting actuation-based applications. The design of the proposed scheme is inspired by the beamforming technique used in radio frequency (RF) communication systems, which attempts to direct a boosted version of the original signal towards a intended receiving node. The proposed system consists of several sensors (Txs) and two actuators (Rxs). The main idea is to activate one Rx at a time through signals emitted from the Txs, which are in fact delayed in order for their peaks to overlap for ensuring a boosted signal at the Rx side. Since the sensors are fallible and prone to errors, it is claimed that if their number is increased, the accuracy of the network is improved. Several design principles are introduced in order to optimize the scheme, and an analytical modelling for calculating the actuation error rate is provided. Then, the simulation results are verified through this analytical solution. The technique is firstly presented for a simplified scheme where the Txs are forming a uniform linear array (ULA), and then the idea is verified for a random topology as well. The actuation accuracy derivation is given for several cases as well, depending on the application where beamforming is utilized. This proposed technique can find application in different areas where actuation of nanomachines is required.

The rest of this dissertation is organized as follows. Chapter 2 focuses on the single-input single-output (SISO) topology and the analytical foundation of MC, as well as a detailed literature review on relaying in MC. The first two contribution works are presented in Chapter 3 and 4, respectively, followed by the molecular beamforming technique, which is investigated in Chapter 5. Lastly, Chapter 6 summarizes and concludes this thesis.

Three journal papers are produced as a result of the contributions of this dissertation. The asymmetrical relaying in MC work has been published in the Institute of Electrical and Electronics Engineering (IEEE) *Transactions on NanoBioscience* (TNB). The optimal relaying in MC work has been accepted for publication in the *Nano Communication Networks* journal. The molecular beamforming study is currently under revision.

Chapter 2

SISO TOPOLOGY AND LITERATURE REVIEW ON RELAYING IN MC

As aforementioned in the previous chapter, MCvD is amongst the most efficient and effective methods for transmitting the information between two terminal nodes in MC. In order to understand the peculiar nature of this paradigm, the simplest scheme is considered, consisting of one Tx and one Rx nodes (SISO).

In this chapter, the SISO scheme is investigated, focusing on the modelling of its channel response, which is the analytical foundation of the literature on MC. Afterwards, a detailed literature review focusing on relaying in MC is provided.

2.1 SISO Topology

Most of the works in the literature use the point model for the Tx, from where the emission of molecules is done and the Rx is usually considered to be spherical with absorbing characteristics. An illustration is provided in Figure 2.1, where the dark blue sphere represents the Tx and the light blue one the Rx node. The emission of molecules is assumed to be done at $t = 0$ s, and the signal shape in the right side is a representation of the received molecules at Rx as a function of time. As it can be seen from the received signal's shape, the molecules propagate towards the Rx, where they start to get absorbed after $t = 0$. The number of received molecules reaches a peak, and then the hitting rate gradually reduces. Next, the analytical derivation of the channel response is presented.

2.1.1 Channel Modelling

Let the distance from Tx to the center of Rx be denoted with r_0. The molecules emitted from the point Tx follow the Brownian motion in their way towards the Rx,

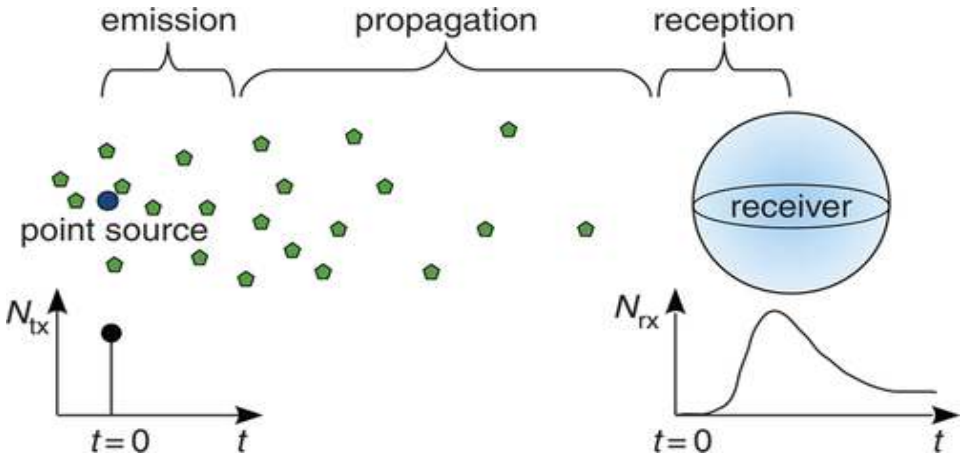

Figure 2.1: MCvD SISO system model [Yilmaz and Chae, 2014a]

which has a radius denoted by r_r. The Brownian motion in the three-dimensional (3-D) environment can be modeled by a random position change (Δx, Δy, Δz), with a normal distribution $\mathcal{N}(0, 2Ddt)$ of zero mean and $2Ddt$ variance, where dt and D denote the time step and the diffusion coefficient, respectively [Dürr et al., 1981]. The position of each molecule for each time step is calculated as below:

$$\begin{aligned} x(t_n) &= x(t_{n-1}) + \Delta x, \\ y(t_n) &= y(t_{n-1}) + \Delta y, \\ z(t_n) &= z(t_{n-1}) + \Delta z, \end{aligned} \tag{2.1}$$

where $(x(t_n), y(t_n), z(t_n))$ denotes the present coordinates, $(x(t_{n-1}), y(t_{n-1}), z(t_{n-1}))$ denotes the previous coordinates and $(\Delta x, \Delta y, \Delta z)$ stands for the position displacement.

The derivation of the hitting rate of molecules absorbed by Rx is given in [Yilmaz et al., 2014]. Fick's second law of diffusion in a 3-D environment, given as:

$$\frac{\partial p(r, t|r_0)}{\partial t} = D\nabla^2 p(r, t|r_0), \tag{2.2}$$

is used for this derivation, where $p(r, t|r_0)$ is the molecule distribution function at time t and distance r, given an initial distance of r_0 and ∇^2 denotes the Laplacian operator. In order to obtain the hitting rate of molecules, initial and boundary conditions are defined in [Yilmaz et al., 2014], following from the assumptions

made in the definition of the system. Then, calculus and probability theory are used to define the hitting rate of molecules as follows:

$$n_{hit} = \frac{r_r}{r_0}\frac{1}{\sqrt{4\,D\,t\,\pi}}\frac{r_0 - r_r}{t}e^{\frac{-(r_0-r_r)^2}{4\,D\,t}}, \tag{2.3}$$

The fraction of molecules received by time t is found by integrating (2.3) from $t'=0$ s to $t'=t$ s, given as:

$$F_{hit}(r_r, r_0, t) = \frac{r_r}{r_0}\text{erfc}\left(\frac{r_0 - r_r}{\sqrt{4\,D\,t}}\right), \tag{2.4}$$

where erfc$(\cdot)$ is the complementary error function. Using (2.4), the expected number of molecules absorbed by Rx for a time interval $[t, t+\Delta t]$ can be evaluated as below:

$$E[N^{Rx}(t, t+\Delta t)] = M^{Tx}\big(F_{hit}(r_r, r_0, t+\Delta t) - F_{hit}(r_r, r_0, t)\big), \tag{2.5}$$

where N^{Rx} denotes the number of molecules absorbed by Rx and M^{Tx} the number of molecules emitted from Tx.

Table 2.1: The parameters used for the SISO scheme simulation.

Parameter	Value
r_0	10 μm
r_r	5 μm
M^{Tx}	10e5
Δt	1e-3 s
D	79.4 $\mu m^2/s$

Next, the simulation results obtained for a SISO scheme with the parameters given in Table 2.1 are compared with the analytical results from the channel modelling derivation presented above. Here, Δt represents the time step used in the simulation for the change in the coordinates of the molecules. The hitting rate of molecules as a function of time, also known as the probability density function (PDF) curve scaled by M^{Tx}, is presented in Figure 2.2. The cumulative distribution function (CDF) curves are presented in Figure 2.3. As seen from these graphs, there

is a slight mismatch between the analytical and simulation curves, which can be reduced by decreasing Δt for improving the accuracy, which comes at the cost of computationally expensive simulation results.

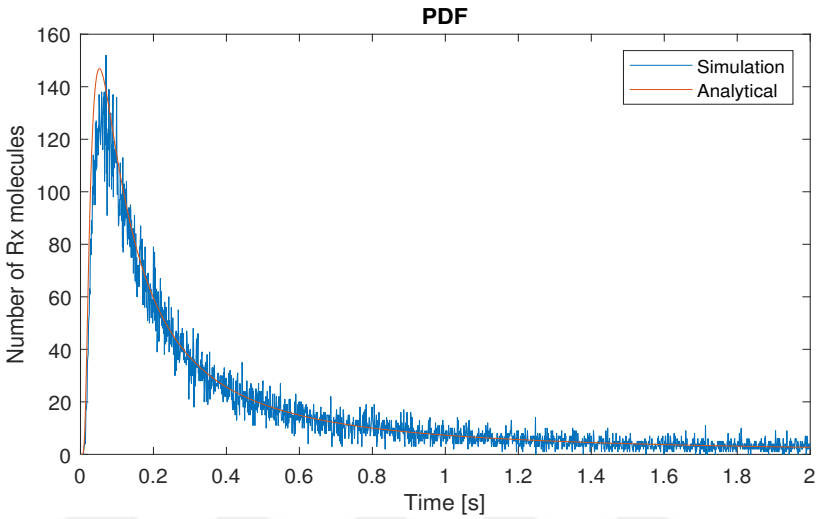

Figure 2.2: The PDF curves for the SISO scheme obtained analytically and from computer simulation.

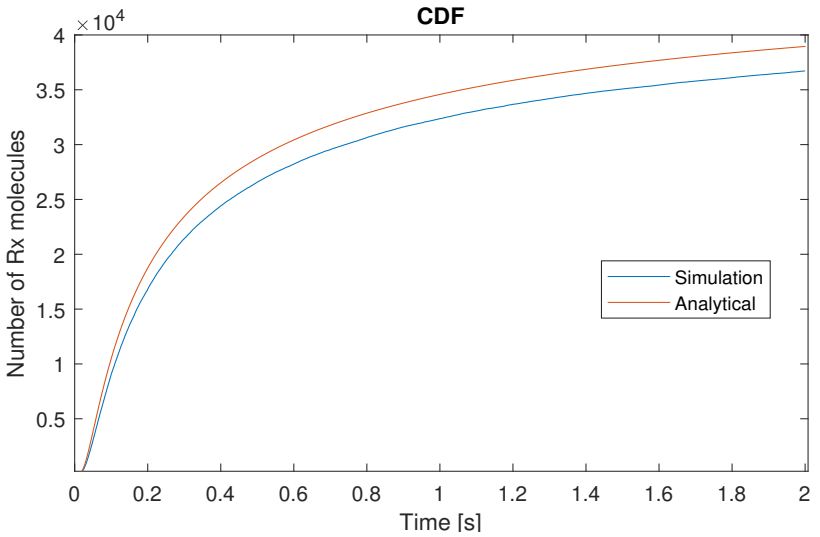

Figure 2.3: The CDF curves for the SISO scheme obtained analytically and from computer simulation.

In MCvD, the molecules are released in an instant, however, they are absorbed by the Rx over time. As earlier discussed, this leads to ISI. Back to Figure 2.1, ISI can be illustrated by the gradual decay of the received signal. This means that the released molecules for a single symbol affect the upcoming symbols as well. The channel coefficients (taps) for a system with channel memory $L = 10$ and symbol duration $T_s = 0.2s$ are shown in Figure 2.4. The channel memory means in fact that the effect of the molecules released for a symbol is affecting the next 9 symbols as well. As seen from the figure, the first tap is dominating, meaning that most of the received molecules are absorbed in the intended symbol time, and then this fraction drops off as time passes, as it was previously illustrated in Figures 2.1 and 2.2. These channel taps can be used to evaluate the performance of the MCvD system, since it is clear that ideally, the first channel tap should be at the possible maximum, and the next ones should have values as close to zero as possible. In the next subsection, the performance in terms of BER is summarized.

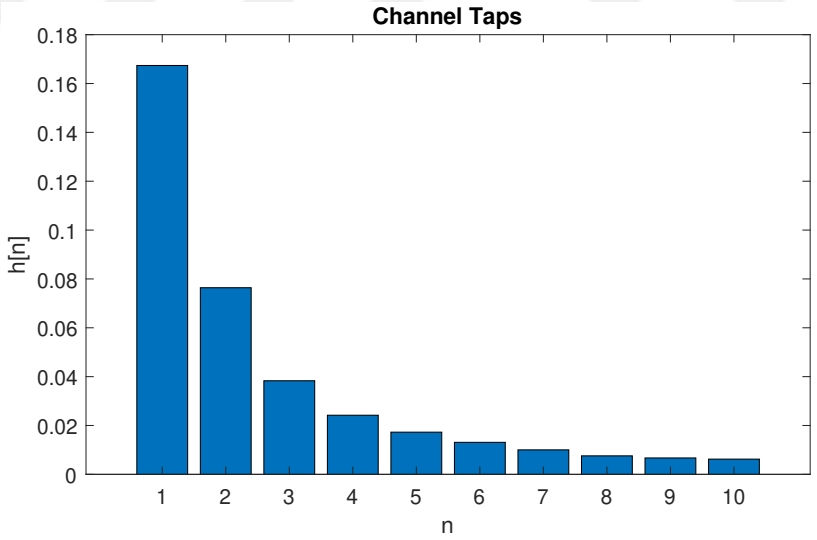

Figure 2.4: The channel taps for the SISO scheme obtained from computer simulation.

2.1.2 BER Derivation

Each molecule arriving at the Rx during the $[t, t + \Delta t]$ time interval can be considered as a success event which occurs with some probability, say $p_t^{t+\Delta t}$. In other words, the reception of each molecule can be considered as an independent binomial process. The authors of [Yilmaz and Chae, 2014a] derive two approximations for modelling the absorbed molecules by Rx, as follows. The Poisson approximation for the received molecules during the $[t, t + \Delta t]$ time interval is given as:

$$N^{Rx}[t, t + \Delta t] \sim \mathcal{P}(M^{Tx} \times p_t^{t+\Delta t}), \tag{2.6}$$

where $\mathcal{P}(\lambda)$ denotes the Poisson distribution with λ mean. The Poisson distribution can be approximated using the Gaussian distribution, which leads to modelling the received molecule number as following:

$$N^{Rx}[t, t + \Delta t] \sim \mathcal{N}(M^{Tx} \times p_t^{t+\Delta t}, M^{Tx} \times p_t^{t+\Delta t} \times (1 - p_t^{t+\Delta t})), \tag{2.7}$$

where $\mathcal{N}(\mu, \sigma^2)$ denotes the Gaussian distribution with μ mean and σ^2 variance.

Equation (2.7) and the channel taps (which represent the probability values of the molecules arriving at Rx) are used to evaluate the BER performance of the scheme versus different M^{Tx} values. For this study, OOK modulation is used, meaning that Tx will emit M^{Tx} molecules for bit-1 and it will stay quiet for bit-0. Then, the demodulation is done by comparing the received number of molecules with a threshold value. As expected, and as seen from Figure 2.5, BER gradually decreases as M^{Tx} increases.

2.2 Relaying in MC

The amplitude of the received signal in MCvD systems is shown to be inversely proportional to the third power of the distance of transmission [Llatser et al., 2011]. Relaying in MC has received a significant interest by researchers, especially due to this long-range communication challenge. This issue further complicates when there are other molecule types apart from the ones used for transmitting information in the surrounding environment [Einolghozati et al., 2013]. In other words, relaying has been proposed to enhance both the reliability and efficiency of MCvD systems.

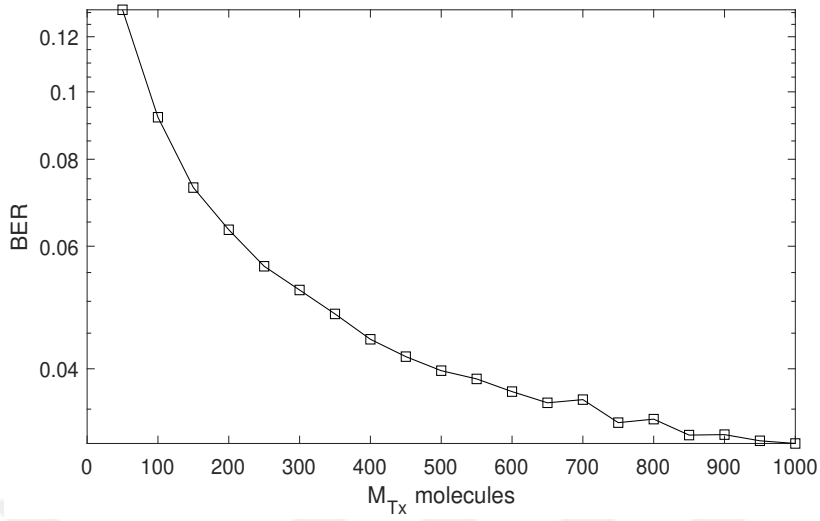

Figure 2.5: BER versus number of transmitted molecules for the SISO scheme.

The idea of repeaters for the issue of signal attenuation is studied by [Nakano and Shuai, 2011], where the design of repeaters is examined in calcium junction channels. Relaying in MCvD has been in fact studied in a variety of schemes and designs, in terms of the functions executed by the relay node, its operation, the utilized modulation schemes etc. For example, the relay may simply decode the received signal and then forward it, or it may amplify the signal for increasing reliability. Some works consider improving the MCvD systems in terms of ISI by enabling the relay node to emit different molecule types than the Tx node. Various modulation techniques have been studied as well, with the purpose of minimizing the error rates and losses of the proposed systems. This section focuses on providing a literature review on the current works and directions on the relay-based MCvD systems.

The authors of [Wang et al., 2017] analyze the performance of an MCvD system, in which the relay decodes and amplifies the signal before forwarding it. Different signal detection methods are investigated, showing that for a channel with drift velocity, minimum error probability (MEP) criterion performs the best. Some key parameters that are directly related to the system's performance have been investigated as well, such as the number of emitted molecules, location of the relay and

Rx's radius. Amplify-and-forward (AF) scheme is also studied in [Ahmadzadeh et al., 2015a]. Here, the authors focus on the derivation of the optimal amplification factor utilized by the relay.

In order for not increasing the cost of utilized molecules, other works based only on information decoding are proposed. An estimate-and-forward (EF) scheme is proposed in [Tiwari and Upadhyay, 2017], in which maximum likelihood estimation is used to estimate the number of emitted molecules. In this case, the performance of the system is boosted while keeping the molecules budged unchanged. Decode-and-forward (DF) scheme is studied in [Wang et al., 2021] as well. In this work, depleted molecule shift keying (D-MoSK) modulation technique is utilized, for which different molecule types are used for transmission. Meanwhile, the authors of [Wang et al., 2015] propose the utilization of time-dependent molecular concentrations for encoding the information, thus taking into consideration both noise and channel memory. The relay then decodes and forwards the information using the same or different type of molecules than those of the Tx. Additionally, this time-dependent scheme comes of help for ISI mitigation at the Rx side. Molecule information and energy transfer is studied by the authors of [Deng et al., 2016]. Here, apart from decoding the information it receives, the relay is able to generate its emission molecules by means of chemical reactions. In [Ghazani et al., 2016], the authors propose a physical layer network coding scheme that utilizes the reaction of the transmitted molecules between each other. The results show that the error probability for the considered two-way relay scheme is decreased, while achieving low complexity though the reaction-based implementation.

In addition to the aforementioned schemes, multi-hop networks with several relays are considered in [Ahmadzadeh et al., 2015b]. Full-duplex and half-duplex modes of transmission are analyzed, and it is found that ISI can be mitigated if the decision threshold for decoding is selected in an adaptive manner. Moreover, closed-form expressions for the error probability of the overall network are provided. Similarly, multi-hop MC is investigated for applications concerned with target detection in [Yang et al., 2019]. Both analytical and simulation results demonstrate that target detection accuracy is increased with the addition of relay nodes. A through-

put improvement by incorporating cooperative relaying in MC is demonstrated by the experimental results of [Alshammri et al., 2018], whereas its augmentation in the gain is proven by the analytical and simulation results in [Yin et al., 2017].

This thesis proposes two novel relay-based schemes, with the purpose of enhancing the performance of MCvD in applications that include longer distance communications. The two following chapters provide the motivation and details of these schemes.

Chapter 3

ASYMMETRICAL RELAYING IN MOLECULAR COMMUNICATIONS

3.1 Motivation

A number of studies in the literature have focused on the optimization of the relay location. For instance, in [Ardeshiri et al., 2017], three nanomachines are located on a straight line and it is found that the best performance is obtained when the relay is placed in the middle of the system. A similar conclusion is drawn in [Yuan et al., 2018]. Meanwhile, the authors of [Wang et al., 2015] investigate the scenario when three nanomachines are not located on a straight line and the effects of the placement angle are discussed. An optimization problem on the matter is proposed in [Tavakkoli et al., 2017], considering a cooperative communication system. The authors of [Wang et al., 2019] study the effects of the relay's position on the BER performance of an AF relay scheme. As the relay approaches the Rx node, the BER increases, because the first-hop signal (Tx to relay) strongly attenuates as a result of the distance. Two different cases of relaying in MCvD systems are investigated in [Jamshidi et al., 2019]: Rx decodes the signal based on the molecules absorbed from the relay only, and then based on the molecules absorbed from the relay and Tx as well, respectively. The optimal relay location for the first scenario is in the middle of the Tx-Rx pair, but this does not hold for the second scenario.

The majority of the works in the literature consider symmetric scenarios in terms of the position of the relay. Nonetheless, practical scenarios might be prone to asymmetries, resulting in different error performances among the communication links established through the relay. As the main purpose of the relay is to enable communication between distant nanomachines, such systems are exposed to error propagation. This results from the fact that the channel of the nanomachine closer

to the relay is of higher quality compared to the further one. In other words, unequal error protection of the MC links leads to a reduced overall performance. In order to alleviate this issue, this work focuses on an asymmetric relay-based scenario, in which the two communicating nanomachines emit molecules with different diffusion coefficients. The main idea is to optimize the system's parameters in such a way that equal error protection is achieved for these two independent links established between two Tx nodes and the relay. In particular, this work focuses on the quality of the communication links from Tx to the relay (uplink, UL). Since the diffusive channel characteristics are the same for the UL and the downlink (DL), the results are expected to hold for the latter as well.

In the literature, the positions of the nanomachines are widely assumed to be fixed. There are also several studies focusing on the impact of the mobility of the nanomachines on the performance of the system, such as [Chouhan and Sharma, 2020] and [Gürsoy et al., 2017]. However, this work also assumes that the Txs and the relay nodes are stationary.

The main contributions of this study are the design of a novel asymmetrical relay system, two different parameter optimization models for this setup, and performance analysis of the proposed solutions.

3.2 System Model

The proposed scenario is illustrated in Figure 3.1, where the orange sphere demonstrates the relay node and the independent point Txs are shown in blue. r_{01} and r_{02}, the distances from the center of the relay to the two Txs respectively, have different values, and the same T_s is utilized for both Txs in order to keep the complexity at a moderate level and achieve synchronous communications. The closer Tx has an advantage compared to the further one, because the molecules that it emits have to travel a shorter distance to reach the Rx (relay). In order to achieve an overall good quality and fair communication, two parameter optimization methods are proposed for the UL in the following section. These methods aim to improve the quality of the further Tx's communication link.

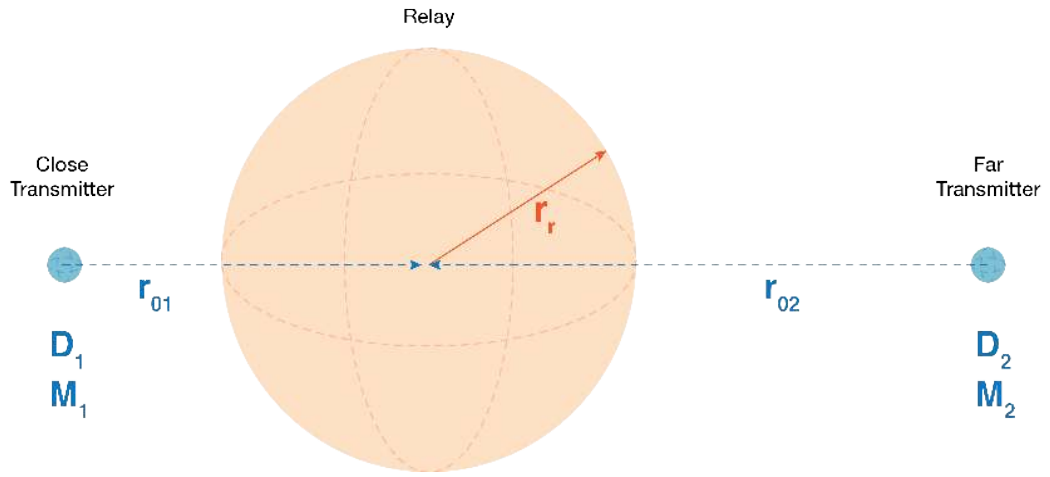

Figure 3.1: Asymmetric communication links of a relaying system, where the independent point Txs are shown in blue and the relay node is the orange sphere.

3.3 Parameter Optimization for Asymmetric Molecular Links

As discussed in the earlier sections, relay schemes are exposed to error propagation, so equal error protection is required for increasing communication reliability of the relay schemes. In order to achieve this for asymmetrical links, the parameters of the two Txs should be optimized such that similar performances are achieved for the Txs. While different approaches may be possible to attain this, this work proposes minimizing the difference between the received signals from the two Txs, which are given from the following formulations:

$$F_{hit_1}(r_r, r_{01}) = M_1 \frac{r_r}{r_{01}} \text{erfc}\left(\frac{r_{01} - r_r}{\sqrt{4\,D_1\,T_s}}\right), \tag{3.1}$$

$$F_{hit_2}(r_r, r_{02}) = M_2 \frac{r_r}{r_{02}} \text{erfc}\left(\frac{r_{02} - r_r}{\sqrt{4\,D_2\,T_s}}\right). \tag{3.2}$$

Here; M_1, D_1 and M_2, D_2 are the respective number of molecules and diffusion coefficient values utilized by the two Txs. The proposed optimization is a diffusion coefficient based approach. Additionally, in order to achieve fairness, it is possible to allow the Tx placed at a further distance to emit a higher number of molecules compared to the other one. Given these suggestions, two different optimization

algorithms for the UL of the relaying system are proposed; one varying the diffusion coefficient D_2 only, and the other one varying D_2 and M_2 simultaneously.

3.3.1 Optimization problem considering D_2 only

Since the squared error is an amenable technique used in optimization problems, the first presented approach aims to minimize the squared error between the two received signals represented in (3.1) and (3.2), given as

$$\epsilon = \left(M_1 \frac{r_r}{r_{01}} \text{erfc}\left(\frac{r_{01} - r_r}{\sqrt{4\, D_1\, T_s}} \right) - M_2 \frac{r_r}{r_{02}} \text{erfc}\left(\frac{r_{02} - r_r}{\sqrt{4\, D_2\, T_s}} \right) \right)^2. \tag{3.3}$$

The first derivative of (3.3) with respect to D_2 is taken and the equation is solved for D_2. Assuming that r_r, r_{01}, r_{02}, T_s and D_1 are known values, and considering $M_1 = M_2$, D_2 can be found as

$$D_2 = \frac{\left(\dfrac{r_{02} - r_r}{\text{erfc}^{-1}\left(\dfrac{r_{02}}{r_{01}} \text{erfc}\left(\dfrac{r_{01} - r_r}{\sqrt{4\, D_1\, T_s}} \right) \right)} \right)^2}{4\, T_s}. \tag{3.4}$$

In other words, improving the performance of the further Tx with respect to the one of the closer Tx can be done by allowing the former to transmit molecules with diffusion coefficient value D_2 computed by (3.4).

3.3.2 Optimization problem considering both D_2 and M_2

Next, this work presents the second optimization problem that accounts for both D_2 and M_2 parameters. The further Tx is enabled to use these two parameters for reaching the performance of the closer Tx. In order to find the pair of values of the unknown parameters for which (3.3) reaches its minimum value, Newton's algorithm for unconstrained optimization is utilized, as given in [Dennis Jr and Schnabel, 1996]. The followed steps are presented in Algorithm 1.

Algorithm 1 Optimizing D_2 and M_2.

Input: r_r, r_{01}, r_{02}, T_s. D_1, M_1, *error_tolerance*

Output: M_2, D_2

1: f: squared error of (3.1) and (3.2) as a function of D_2, M_2

2: $\epsilon = f(\mathrm{D}_2, M_2)$

3: Define K as

$$K = \frac{\partial^2 f}{\partial M_2^2}\frac{\partial^2 f}{\partial D_2^2} - \left(\frac{\partial^2 f}{\partial D_2 \partial M_2}\right)^2$$

4: **while** $\epsilon >$ *error_tolerance* **do**

5:

$$(M_2)_{n+1} = (M_2)_n - \frac{|A|}{K((M_2)_n, (D_2)_n)}$$

6:

$$(D_2)_{n+1} = (D_2)_n - \frac{|B|}{K((M_2)_n, (D_2)_n)}$$

7: Update ϵ

8: **end while**

In Algorithm 1, $|A|$ and $|B|$ denote the respective determinants of the following matrices

$$A = \begin{pmatrix} \frac{\partial^2 f}{\partial D_2^2}((D_2)_n,(M_2)_n) & \frac{\partial^2 f}{\partial M_2 \partial D_2}((D_2)_n,(M_2)_n) \\ \frac{\partial f}{\partial D_2}((D_2)_n,(M_2)_n) & \frac{\partial f}{\partial M_2}((D_2)_n,(M_2)_n) \end{pmatrix}$$

$$B = \begin{pmatrix} \frac{\partial^2 f}{\partial M_2^2}((D_2)_n,(M_2)_n) & \frac{\partial^2 f}{\partial M_2 \partial D_2}((D_2)_n,(M_2)_n) \\ \frac{\partial f}{\partial M_2}((D_2)_n,(M_2)_n) & \frac{\partial f}{\partial D_2}((D_2)_n,(M_2)_n) \end{pmatrix}$$

Here, n represents the current iteration, and *error_tolerance* is a predefined parameter that affects the accuracy and preciseness of the obtained results. An adequate initialization of M_2 and D_2, by taking into consideration the overall parameters of the system, can result in a faster convergence towards the final optimized values.

3.4 Simulation Results

Firstly, the case when both Txs emit molecules with the same D value is considered, in order to compare it with the optimized results afterwards. As a starting point, r_{01}, r_{02}, and r_r are selected to be $8.5\mu m$, $10\mu m$, and $5\mu m$, respectively. The Txs are independent and they emit 10^6 molecules with diffusion coefficient value of $39.7\mu m^2/s$ for bit-1, and nothing for bit-0, as OOK modulation is used. The symbol time is selected to be $0.22s$, and the channel memory is 10 taps. At the relay side, demodulation is performed by simple thresholding for each time slot such that the relay decides on bit-1 if it receives more molecules than the threshold, and bit-0, otherwise. The Poisson-distributed environmental noise is considered to be independent of the source signal, with a mean of $\lambda = 2$, as shown in [Arjmandi et al., 2013]. A total of 10^6 bit transmissions are simulated for the BER calculations, and the number of the received molecules is modeled following the Gaussian approximation as shown in [Yilmaz et al., 2015], which is also derived in the previous chapter. The values of the parameters used for the simulations and for the optimization problems are summarized in Table 3.1. The BER performances are obtained using computer simulations in Matlab.

Secondly, the optimization of D_2 is performed. Considering all the aforementioned parameters unchanged, the value of D_2 is found as $110.54\mu m^2/s$ using (3.4).

Table 3.1: The initial parameters used in the simulations and for the optimization problems.

Parameter	Value
r_{01}	8.5 μm
r_{02}	10 μm
r_r	5 μm
M_1	10e6
D	39.7 $\mu m^2/s$
T_s	0.22 s
Channel Memory	10

The BER curves presented in Figure 3.2 are obtained from the two preceding cases for which each Tx has a separate BER curve, since the Txs are independent from each other. It should be noted that the BER curve of the close Tx is not affected by the optimization problems. As observed from this figure, the performance for the closer Tx of the first case is significantly better than the further one, meaning that the performance of this system exhibits unequal error protection for the two Txs. For the second case, it can be observed that there is an improvement of the average BER curve for the two communication links. However, there is still room for improvement as the goal is to reach equal error protection for the two links, or in other words, bringing the average BER curve even closer to the individual ones. For this reason, the second optimization problem is considered. In order to observe the conditions of the two Txs more clearly, the channel coefficients and CDF curves for the two aformentioned scenarios are also presented in Figure 3.3 and 3.4, respectively. It is observed that the error between the two CDF curves is significantly reduced for the optimized D_2 value. As the first optimization solution aims, the first channel taps of the two Txs are matched, which is reflected on their CDF curves as well. The aforementioned improvement on the BER performance of the far Tx is expected, since its first channel tap is increased and the following channel taps,

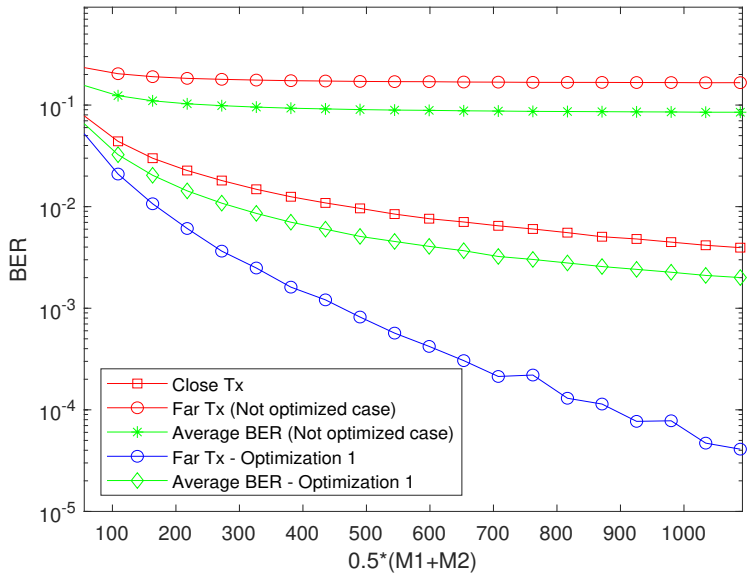

Figure 3.2: BER performances of the two communication links for not optimized parameters and the optimized D_2 case.

which account for ISI, are slightly decreased.

For the third case, the initialization values of M_2 and D_2 are selected to be 10^6 and $79.4\mu m^2/s$, respectively, with the latter being the benchmark value of diffusion coefficient in the literature, whereas all the other parameters are the same as before. After seven iterations, the values converged to $M_2 = 1.17738 \cdot 10^6$ and $D_2 = 80.9126\mu m^2/s$. For the newly obtained values, the CDFs and BER performance of the scheme are illustrated in Figures 3.5 and 3.6, respectively, whereas the channel coefficients are shown in Figure 3.3. It is observed that for these values, the CDF curves and all the channel coefficients for both Txs are equal. This is clearly reflected in the BER performances as well, where the average BER curve is very close to the the curves of the individual molecular links. In other words, the optimized parameters enable the system to achieve equal error protection for both communication links.

As expected, the second optimization problem achieves better results compared to the first one. As mentioned before, these results are expected to hold for the DL as well, since the nature of diffusion is same for both UL and DL.

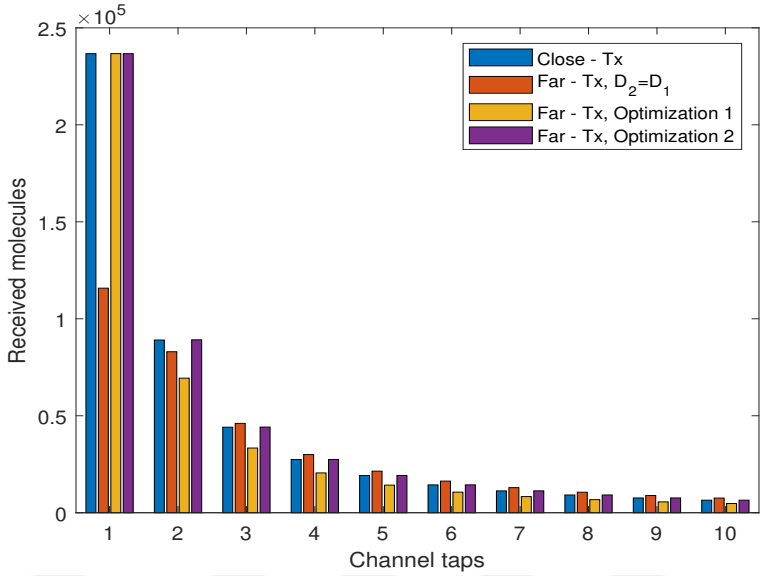

Figure 3.3: Channel coefficients for not optimized and optimized cases.

The initial work explored the optimization of the number of molecules alone as well, since it is easier and more feasible. However, the results showed that the optimization of the diffusion coefficient has more potential than the number of molecules in achieving the goal of equal error protection. As shown in Figure 3.7, optimizing M_2 (number of transmitted molecules from the further Tx) only, gives the worst result among the three considered scenarios. Similarly, in Figure 3.8, it is shown that the quality of the far Tx's link is much worse than that of the close one.

Noting that the diffusion coefficient is not a tuneable parameter, a very good effort in designing the system can be done beforehand in order to perform this optimization solution. As factors such as temperature and viscosity are dependent on the environment characteristics (and are generally considered to be the same for both Txs), molecules with different Stokes radii can be utilized. Molecules that have Stokes radii as close to the optimized one as possible can be chosen in the design process. Since optimizing the diffusion coefficient can be done in a coarse manner, it is possible to utilize it to find a close-to-optimal solution and further fine-tuning can be achieved by adjusting the secondary parameters such as distances, number of transmitted molecules etc.

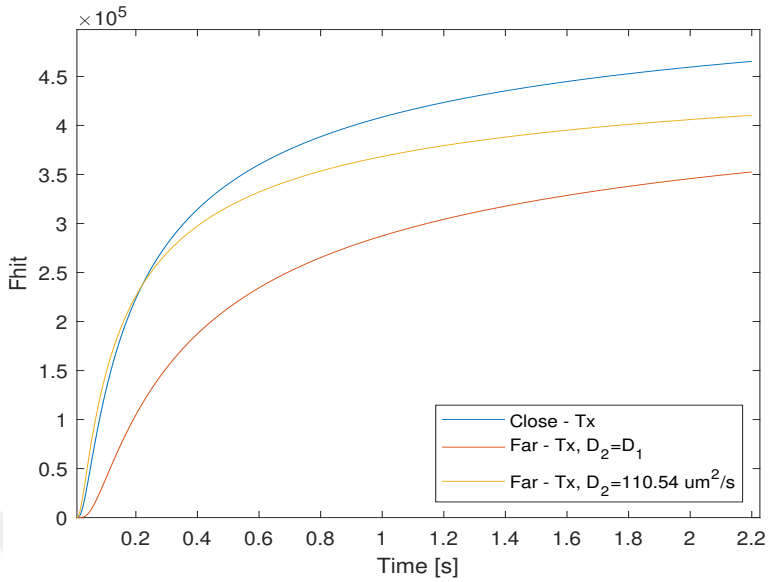

Figure 3.4: CDF curves for not optimized and optimized D_2.

As for the optimized values of D_2 and M_2, the plot in Figure 3.9 shows that when these parameters are jointly optimized, there is a pair of them for which the error between the two received signals reaches to a minimum (shown in red). The values of D_2 and M_2 shown in the plot correspond to the solution given by Algorithm 1. In other words, it is expected that this algorithm gives a unique global solution for this problem.

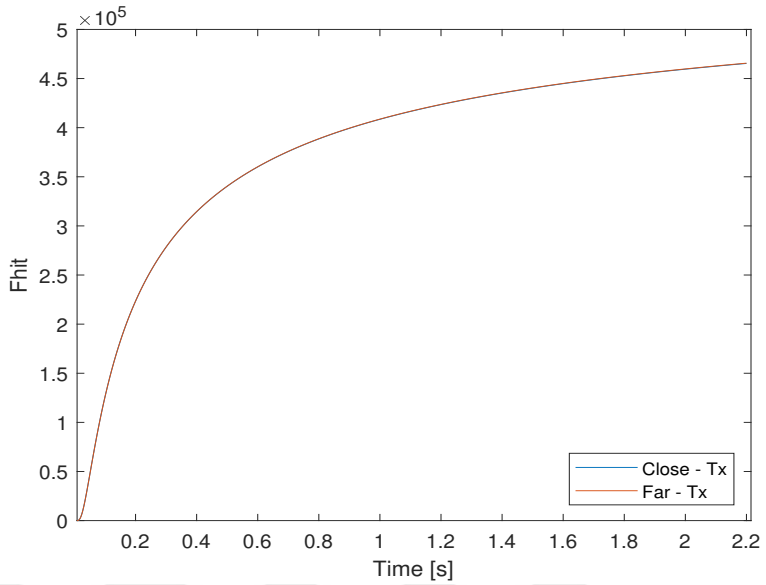

Figure 3.5: CDF curves for optimized D_2 and M_2 values.

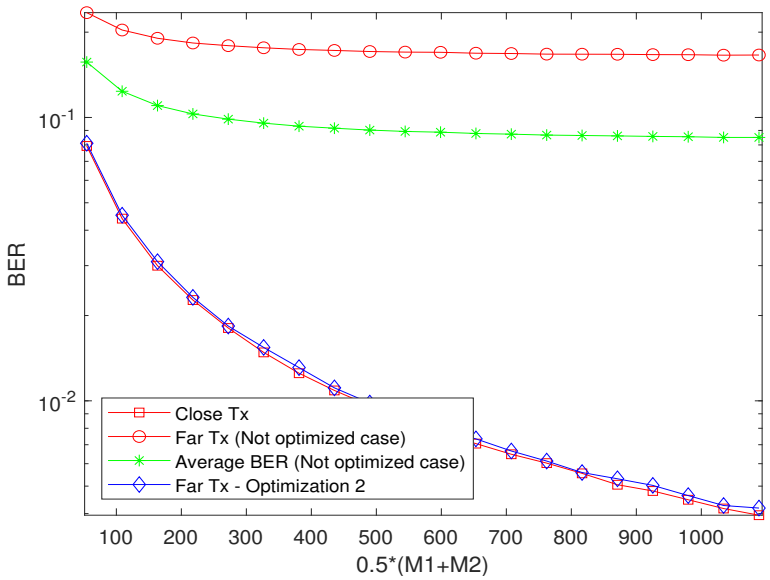

Figure 3.6: BER performances of the two communication links for not optimized parameters and the optimized D_2 and M_2 case.

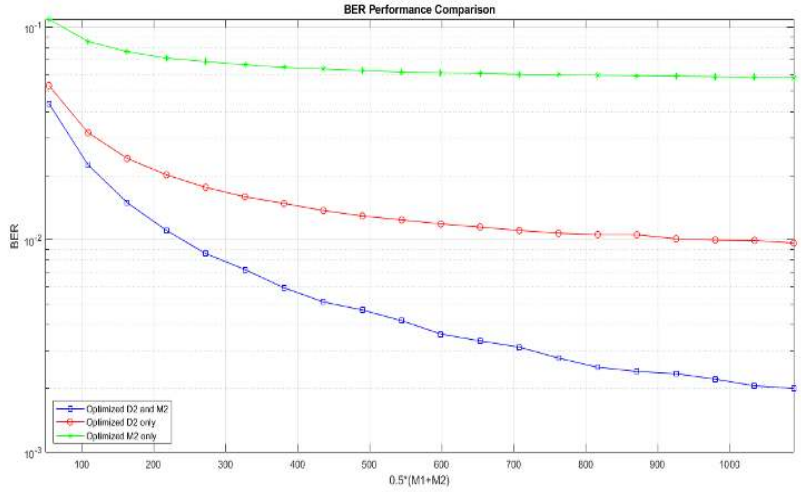

Figure 3.7: BER comparison between for the communication link of the further Tx for optimized M_2 and D_2 alone, and together.

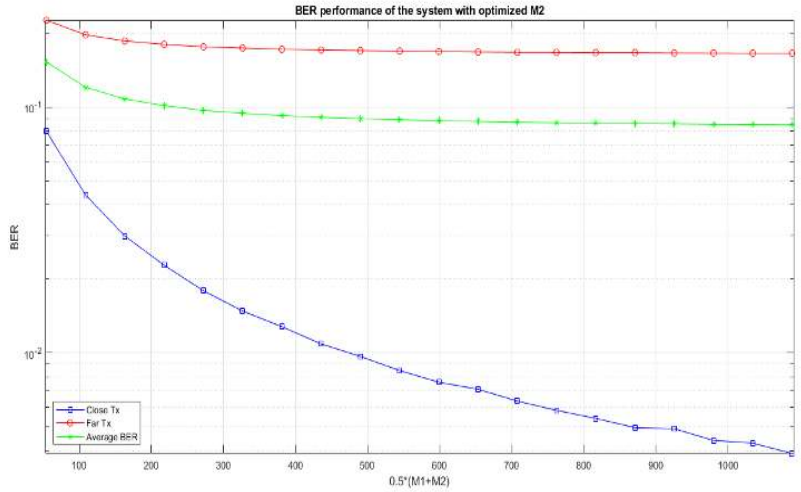

Figure 3.8: BER performance for the two communication links for optimized M_2 alone.

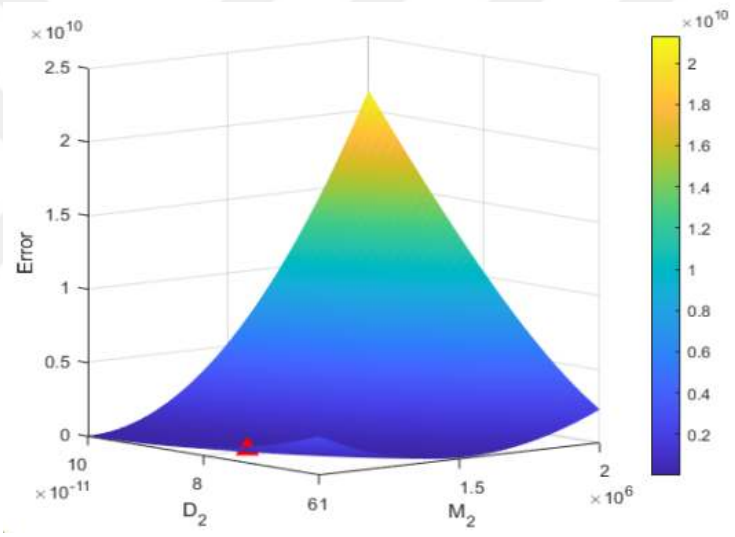

Figure 3.9: Optimization of D_2 and M_2 parameters.

Chapter 4

OPTIMAL RELAYING IN MOLECULAR COMMUNICATIONS

4.1 Motivation

Most of the works in the literature consider molecular relaying with the purpose of extending the communication range between nanomachines, and thus simultaneously decreasing the error rates. Moreover, the SISO communication topology is one of the most studied systems in the MC literature. However, the foreseen applications include smart drug delivery, immune system triggering, etc., which require a network of communication devices coexisting and communicating in the same MC channel. Therefore, it is envisioned that research on MC should evolve from SISO communications to more complicated topologies. Stimulated by the principle of relaying and by the fact that interfering molecules (the ones constituting ISI) arrive at the Rx later than the non-interfering molecules (the ones received during the intended symbol time), in this chapter an optimal MC relaying scheme that aims to enhance the overall performance of the communication link is proposed.

Considering a basic MC scheme that consists of a point Tx and a spherical Rx, the received non-interfering molecules can be roughly thought of as line-of-sight (LoS) molecules, whereas the interfering ones as non-line-of-sight (NLoS) molecules, as roughly illustrated in Figure 4.1. If examined separately, each of those two components has its own peak time of arrival, which can be calculated as explained in [Yilmaz et al., 2014]. In this work, a novel relay-based system that aims to isolate these two components is proposed. The main idea is to introduce a relay to this basic scheme somewhere between the Tx and Rx, which will collect the LoS molecules until a time τ and release them afterwards towards the Rx, such that LoS and NLoS molecules arrive almost at the same time at the Rx. Although there is

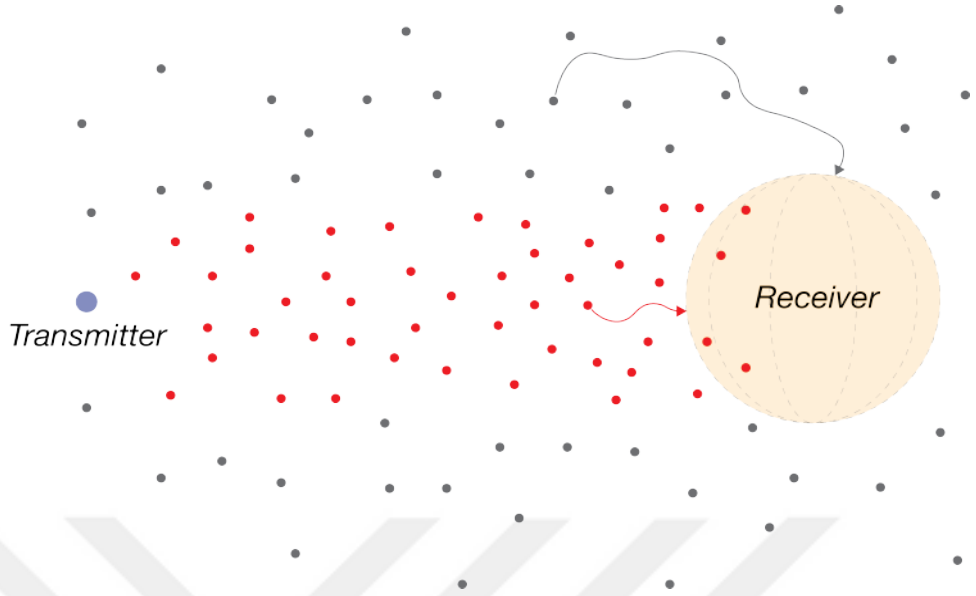

Figure 4.1: A rough illustration of the emitted molecules from the Tx, where the red molecules are the LoS molecules and the grey ones are the NLoS molecules.

a slight communication delay by doing so, this scheme can improve the error rate as well as extend the communication range by enhancing the received signal shape. The concept is inspired by the recent research on reconfigurable intelligent surfaces (RIS) in wireless networks, which aims to enhance the performance of the network by optimally modifying the propagation environment [Basar et al., 2019]. Thus, since the proposed scheme is based on manipulating the received signal's shape, this scheme is addressed as optimal relaying scheme. The received signal gets stronger with the introduction of the relay, since the majority of the molecules arrive at the Rx almost at the same time. To better illustrate this concept, an analogy can be drawn between this scheme and the optical lens: the relay aims to collect the molecules in time, just as the lens collects the beams of parallel rays [Young et al., 1996].

In order to obtain the parameters of the most advantageous scheme, an optimization problem is introduced to find the optimum τ value for which the minimum BER is achieved. τ value is an important parameter, since it directly affects both how much the first channel tap is boosted at the Rx and the ISI level. For this

reason, the optimization problem is based on the optimization function proposed by the authors of [Akdeniz et al., 2018], known as signal to interference difference (SID), whose global maximum corresponds almost to the global minimum of BER. SID is basically the difference between the first channel tap and the summation of all the consequent taps. The validation of this approach is done by comparing the results of the analytical model of the proposed system with the results obtained from the simulations. The BER comparison between the optimal relaying scheme and the conventional SISO model shows the potential improvement that this scheme provides.

4.2 System Model

As mentioned earlier, the conventional MCvD scheme consists of a Tx-Rx pair in a fluid environment and molecules that convey the information. The Tx is a point source, whereas the Rx is a sphere with radius r_0. The distance between the Tx and the center of the Rx is denoted by r_r. When the molecules are emitted in an unbounded 3-D environment without drift, they propagate following the Brownian motion. The portion of molecules absorbed until time t is modeled as in (2.4), which is the cumulative fraction of absorbed molecules (CFAM) by the Rx [Yilmaz et al., 2014]. The proposed scenario is similar to the aforementioned one, the only difference being that a spherical relay is placed between the Tx and the Rx, as shown in Figure 4.2. The radii of the relay and the Rx are denoted by r_{0_1} and r_{0_2}, respectively. The distance from the Tx to the center of the relay is denoted by d_1, the distance from the center of the relay to the center of the Rx by d_2, and $d_3 = d_2 + r_{0_1}$.

Assuming that the molecules are emitted from the Tx at time $t = 0$, the relay absorbs the arriving molecules until $t = \tau$. In the meantime, the Rx node absorbs few NLoS molecules. After a specified delay τ, the relay releases the absorbed molecules simultaneously from the closest point to the Rx. This means that the Rx will be receiving NLoS molecules until time τ, and then molecules arriving from both the Tx and the relay. It is noteworthy to mention that the relay is assumed to be reflective

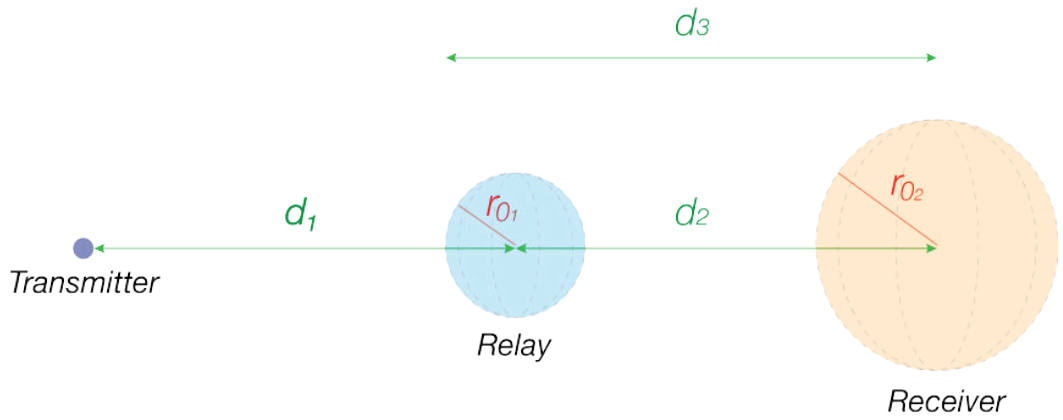

Figure 4.2: Optimal relay-based proposed system, where the relay is between the Tx-Rx pair.

after time τ, such that if the emitted molecules hit back to the surface of the relay, they are reflected back. Considering the transmission of a single bit, the received molecules can be divided into groups for a better understanding of the optimization problem, which will be introduced in the following section. These groups are listed below:

- N - the molecules emitted from the Tx,
- $M_{Tx}^{Rx}\ (0, T_s)$ - the molecules received by the Rx released from the Tx during the first symbol duration (T_s),
- $M_{Tx}^{Rx}\ (T_s, t)$ - the molecules received by the Rx released from the Tx after the first symbol duration, for any time $t > T_s$,
- $M_{Tx}^{Rel}(\tau)$ - the molecules absorbed by the relay until time τ,
- $M_{Rel}^{Rx}\ (\tau, T_s)$ - the molecules absorbed by the Rx released from the relay during the first symbol duration,
- $M_{Rel}^{Rx}\ (T_s, t)$ - the molecules absorbed by the Rx released from the relay after the first symbol duration, for any time $t > T_s$.

In other words, the components corresponding to the desired received molecules are $M_{Tx}^{Rx}\ (0, T_s)$ and $M_{Rel}^{Rx}\ (\tau, T_s)$, whereas $M_{Tx}^{Rx}\ (T_s, t)$ and $M_{Rel}^{Rx}\ (T_s, t)$ constitute the ISI.

The analytical derivation of these terms, as well as the optimization problem, are described in the following section.

4.3 Parameter Optimization

In this section, the analytical approach for obtaining the received signal by deriving the aforementioned components is studied first. Then, the optimization function that is utilized to find the optimum τ value is introduced. It is noteworthy to mention that apart from the τ value, the position of the relay is another crucial parameter that has a direct impact on the performance of the system, since it is directly related to the fraction of the molecules that the relay directs towards the Rx. Joint optimization of both τ and d_1 can be considered in future works.

4.3.1 Analytical Modelling of the System

The time until which the relay delays the LoS molecules (τ) is a crucial parameter for the optimal relaying scheme. If the delay time is very short, the signal is not sufficiently manipulated. On the other hand, if the delay is long, the tail becomes very heavy.

The optimization of τ aims to solve this trade-off and determine the delay for which BER is at minimum. An initial approach for finding τ, based on the relay delaying its release time by the peak times of the LoS and NLoS components (peak times derived as in [Yilmaz et al., 2014]), did not yield the global maximum of SID; thus, BER is not at its minimum. As an alternative approach, SID optimization was considered. In order to obtain the SID optimization function, the previously mentioned signal components should be derived.

The number of molecules absorbed by the relay, released from the Tx at $t = 0$,

can be calculated by

$$M_{Tx}^{Rel}(\tau) = N\frac{r_{0_1}}{d_1}\text{erfc}\left(\frac{d_1 - r_{0_1}}{\sqrt{4\,D\,\tau}}\right), \tag{4.1}$$

assuming that the Rx does not interfere with the molecules between the Tx and the relay in the first τ seconds of the transmission. In other words, the very small fraction of molecules that might be absorbed by the Rx during this time is considered insignificant. Similarly, the number of molecules absorbed by the Rx from the relay can be calculated using

$$M_{Rel}^{Rx}(\tau, T_s) = M_{Tx}^{Rel}(\tau)\frac{r_{0_2}}{d_2 - r_{0_1}}\text{erfc}\left(\frac{d_2 - r_{0_1} - r_{0_2}}{\sqrt{4\,D\,(T_s - \tau)}}\right), \tag{4.2}$$

$$M_{Rel}^{Rx}(T_s, t) = M_{Tx}^{Rel}(\tau)\frac{r_{0_2}}{d_2 - r_{0_1}}\text{erfc}\left(\frac{d_2 - r_{0_1} - r_{0_2}}{\sqrt{4\,D\,t}}\right). \tag{4.3}$$

Although these expressions are due to (2.4), the spherical shape of the relay does not match the point Tx assumption of (2.4), and this leads to an approximation.

Table 4.1: The parameters used for the optimal relay scheme simulation.

Parameter	Value
r_{0_1}	1 μm
r_{0_2}	4.5 μm
d_1	3 μm
d_2	7 μm
T_s	0.35 s
D	79.4 $\mu m^2/s$
τ	0.095 s

The expression in (4.2) is used to calculate the received molecules during the first symbol time, whereas in the expression (4.3), $t > T_s$, so this expression stands for any time interval after the first symbol time. The validity of these expressions are shown in Figures 4.3 and 4.4, where the CFAM and hitting rate of molecules

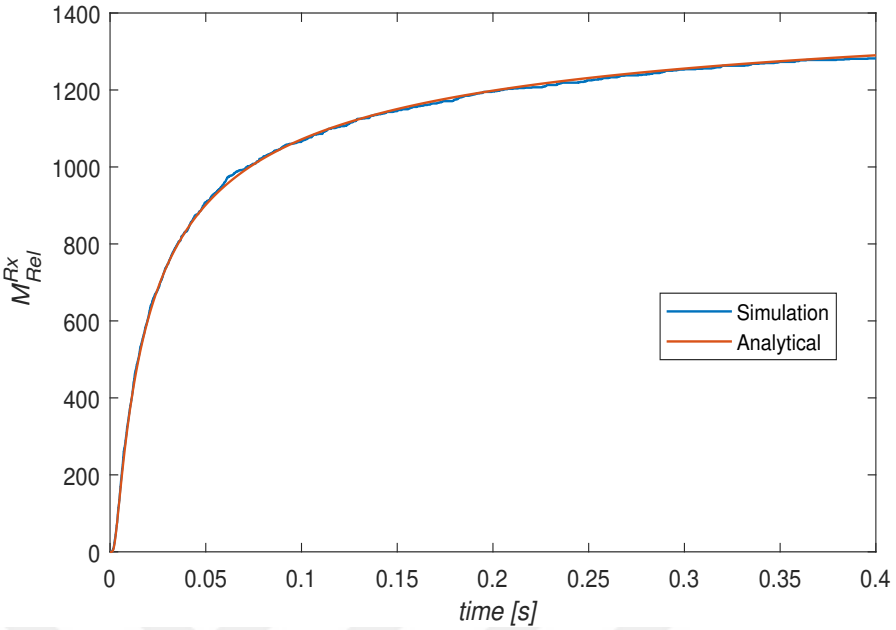

Figure 4.3: Simulation and analytical CFAM curves for the absorbed molecules by the Rx released from the relay.

curves of the analytical model and the simulation results are shown, respectively. It is observed that the absorbed portion of molecules whose source is the relay is modelled quite accurately. Moreover, the reflective characteristic of the relay does not become an impediment towards modelling these components, because its impact is not tremendous. This is because the relay has a finite surface, thus it does not act as an infinite mirror for the molecules that hit the relay back. The values of the parameters of the system for which these graphs are obtained are given in Table 4.1. The selected value of τ in Figures 4.3 and 4.4 is not the optimized one, as the purpose of this section is validating the proposed system model.

The expressions derived so far dealt with the Tx-relay and relay-Rx links, which were not heavily affected by the existence of the third body (Rx and Tx, respectively). On the other hand, the derivation of the expressions for the received molecules whose source is the Tx is not straightforward. This is due to the shadowing effect that originates from the presence of the relay. The authors of [Yaylali et al., 2021] propose an analytical expression for the received molecules for a single-input

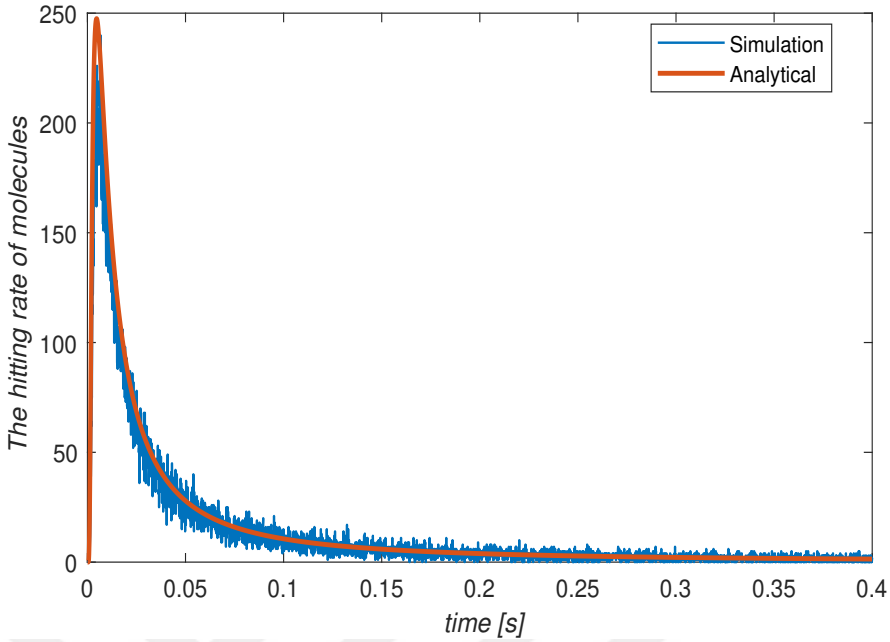

Figure 4.4: Simulation and analytical curves for the hitting rate of the absorbed molecules by the Rx released from the relay.

multiple-output (SIMO) topology, based on the original SISO response. However, the proposed expressions and approximations are heavily affected by the shadowing effect. Since τ is strictly smaller than T_s, consequently being a rather short time, the equations derived in [Yaylali et al., 2021] hold for the proposed scheme reasonably. Based on these expressions, the closest point of the relay to the Rx is considered to be the "virtual" release point, whose distance is included in the $f(t)$ function (d_3). The expression for calculating the number of molecules received from the Tx during any time interval is given as

$$M_{Tx}^{Rx}(0,t) = N\left(\frac{r_{0_2}}{d_1+d_2}\operatorname{erfc}\left(\frac{d_1+d_2-r_{0_2}}{\sqrt{4\,D\,t}}\right)-f(t)\right), \tag{4.4}$$

where

$$f(t) = \begin{cases} \frac{r_{0_1}}{d_1}\operatorname{erfc}\left(\frac{d_1-r_{0_1}}{\sqrt{4\,D\,t}}\right) * \frac{r_{0_2}}{d_3}\operatorname{erfc}\left(\frac{d_3-r_{0_2}}{\sqrt{4\,D\,t}}\right), & 0 < t \leq \tau, \\ \frac{r_{0_1}}{d_1}\operatorname{erfc}\left(\frac{d_1-r_{0_1}}{\sqrt{4\,D\,\tau}}\right) * \frac{r_{0_2}}{d_3}\operatorname{erfc}\left(\frac{d_3-r_{0_2}}{\sqrt{4\,D\,t}}\right), & \text{otherwise.} \end{cases}$$

For instance, considering any time interval after the first symbol duration, the

number of molecules received is calculated as

$$M_{Tx}^{Rx}(T_s,t) = N\Bigg(\frac{r_{0_2}}{d_1+d_2}\text{erfc}\left(\frac{d_1+d_2-r_{0_2}}{\sqrt{4\,D\,t}}\right)- \frac{r_{0_1}}{d_1}\text{erfc}\left(\frac{d_1-r_{0_1}}{\sqrt{4\,D\,\tau}}\right)*\frac{r_{0_2}}{d_3}\text{erfc}\left(\frac{d_3-r_{0_2}}{\sqrt{4\,D\,t}}\right)\Bigg), \tag{4.5}$$

for $t>T_s$.

The corresponding CFAM and hitting rate of molecules curves are shown in Figures 4.5 and 4.6, respectively. Although there is a distinguishable offset between the curves, the preceding approximations fit sufficiently good with the simulation results.

4.3.2 SID optimization function

The next step in this analysis is obtaining the SID function. According to [Akdeniz et al., 2018], SID is calculated as

$$SID = h[1]-\sum_{n=2}^{L} h[n], \tag{4.6}$$

where $h[n]$ is the channel tap for the n^{th} symbol duration and L is the channel memory. The computation of the first channel tap for the considered scenario is given as

$$h_\tau[1] = \frac{M_{Rel}^{Rx}(\tau,T_s)+M_{Tx}^{Rx}(0,T_s)}{N+M_{Tx}^{Rel}(\tau)}. \tag{4.7}$$

The other channel taps are obtained in a similar manner. For calculating the channel taps, the overall number of transmitted molecules is considered in order to fairly evaluate this scheme. When $L\rightarrow\infty$, SID can be rewritten as

$$SID(\tau) = h_\tau[1]-\sum_{n=2}^{\infty} h_\tau[n] \;\; = 2h_\tau[1]-\frac{M_{Rel}^{Rx}(T_s,\infty)+M_{Tx}^{Rx}(T_s,\infty)}{N+M_{Tx}^{Rel}(\tau)} \tag{4.8}$$

The above SID function is the objective function, which needs to be maximized to obtain the optimal τ value. The τ value for which SID reaches its maximum value is found by simulations. The following section summarizes the obtained results and points out the advantages of this scheme compared to a simple MCvD scenario.

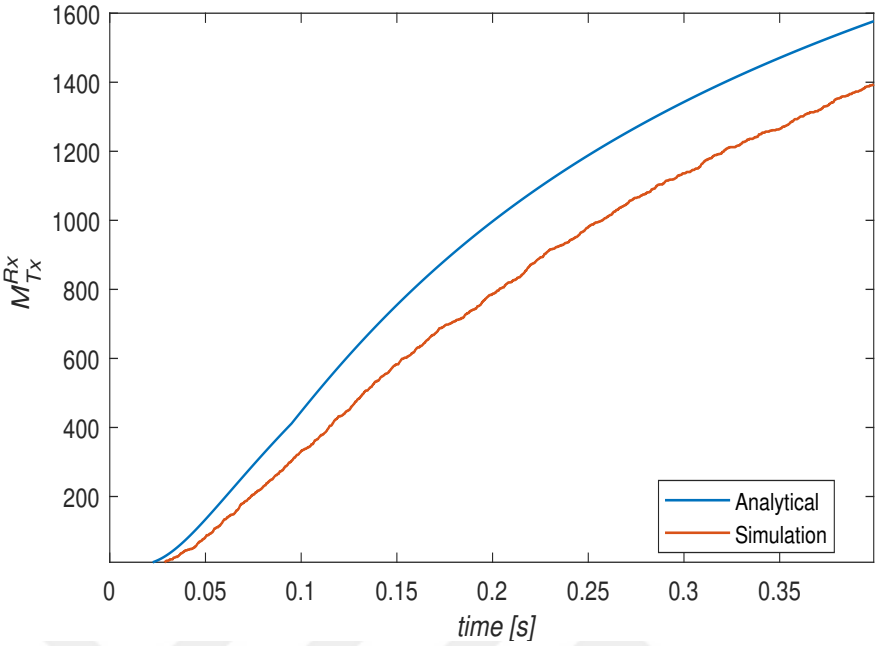

Figure 4.5: Simulation and analytical CFAM curves for the absorbed molecules by the Rx released from the Tx.

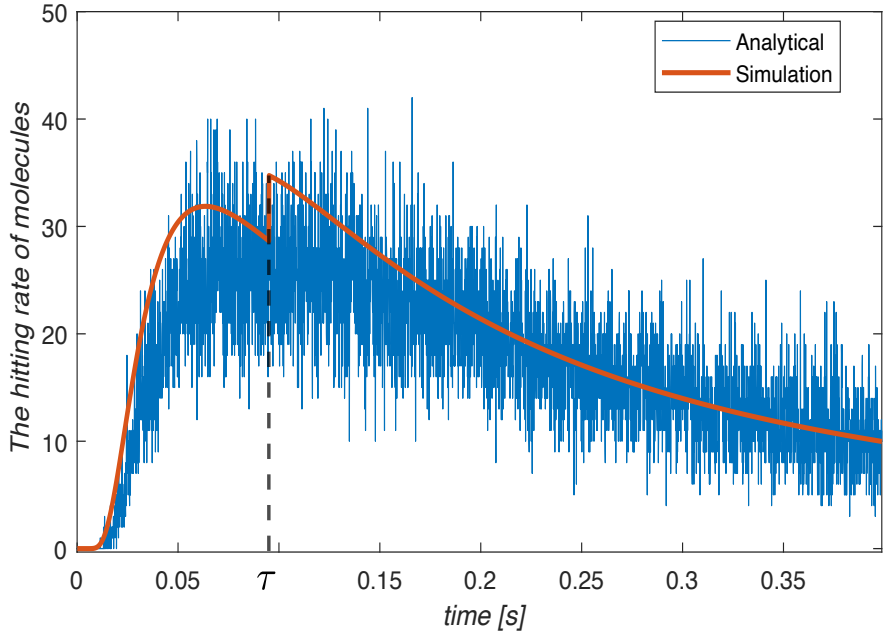

Figure 4.6: Simulation and analytical curves for the hitting rate of the absorbed molecules by the Rx released from the Tx.

4.4 Simulation Results

The validation of the model is done by comparing the results obtained from the analytical SID expression with the ones acquired from computer simulations. The analytical model considers infinite channel memory, whereas the simulations are performed for $L = 50$, which is a quite accurate representation of the infinite MCvD channel. The following results correspond to the evaluation of the optimal relaying scheme for the parameters listed in Table 4.1.

Firstly, the two curves shown in Figure 4.7 are the analytical and simulation results of the computation of the SID function. Although there is a difference between the two curves, their maximum values are achieved for the same value of $\tau = 0.11s$. The reason behind the difference between these curves might come as a result of the slight separation shown in Figure 4.5, thus from the fact that the analytical modelling of the scheme is based on assumptions that lead to approximations. However, it is important that the optimal performance is obtained for the same τ value both analytically and through simulations, Apart from that, the minimum BER value is also obtained for the same τ value, as shown in Figure 4.8. This curve is obtained from the simulation results, for a fixed transmitted number of molecules, $M_{Tx} = 10^6$. As can be seen, the SID-simulation curve and the BER curve are almost mirroring each other, which once again demonstrates that SID function maximization corresponds to the BER function minimization.

The overall BER performance of this scheme is shown in Figure 4.9. First of all, the improvement that the optimal relaying scheme provides compared to the conventional SISO setting is clear. For any τ value around the optimized one, the achieved BER values are lower compared to the SISO case. Additionally, the optimized value gives the best BER performance amongst them. It should be mentioned that, when plotting these curves, both the molecules transmitted from the Tx and the relay are counted, to make the comparisons with the SISO case fair. The T_s value is also an important parameter in order to provide significant improvement of the received signal. The received signal itself is shown in Figure 4.10 for the optimal relaying scheme presented above and the conventional SISO scheme. As it can be

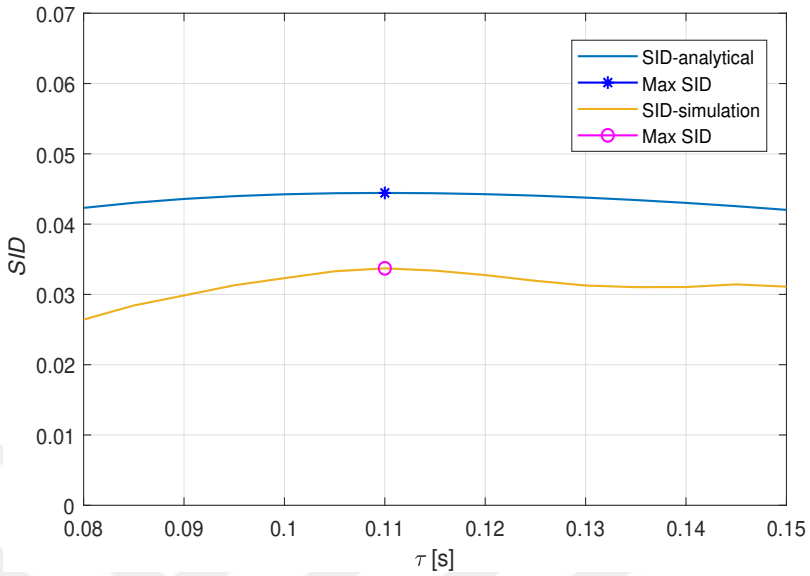

Figure 4.7: SID curves obtained from the analytical model and computer simulations, with both maximum values are reached for $\tau = 0.11s$.

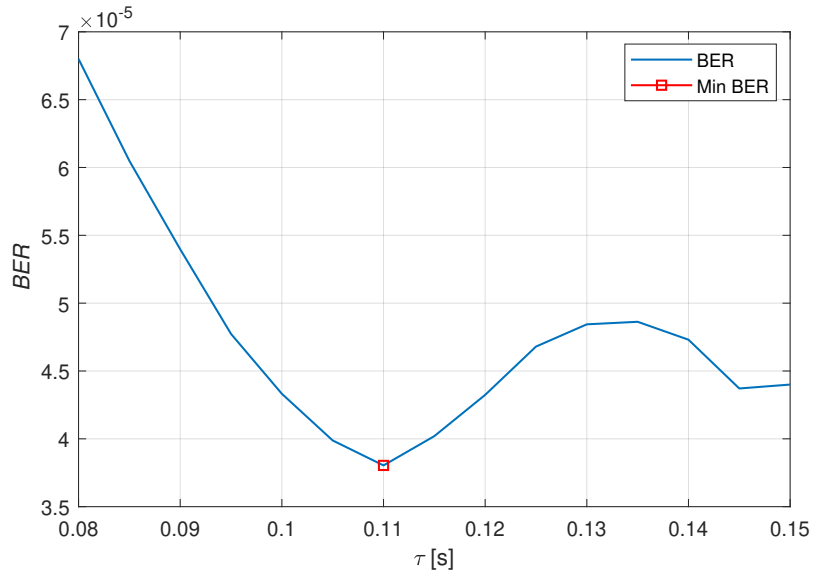

Figure 4.8: BER curve obtained for $M_{Tx} = 10^6$ emitted molecules for the optimal relaying scheme with its minimum value at $\tau = 0.11s$.

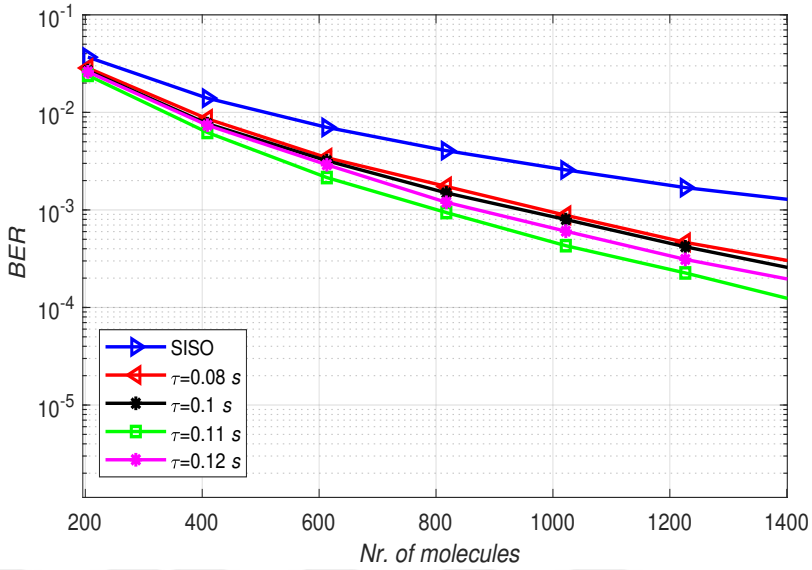

Figure 4.9: Comparison of BER between the optimal relaying scheme with different τ values and the conventional SISO setting.

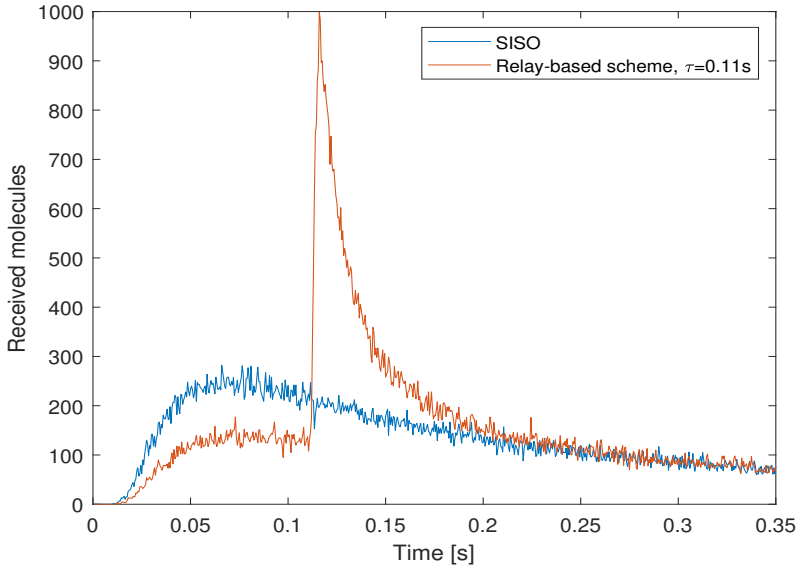

Figure 4.10: Comparison of the hitting rate of molecules for the optimal relaying scheme with $\tau = 0.11s$ and conventional SISO scheme.

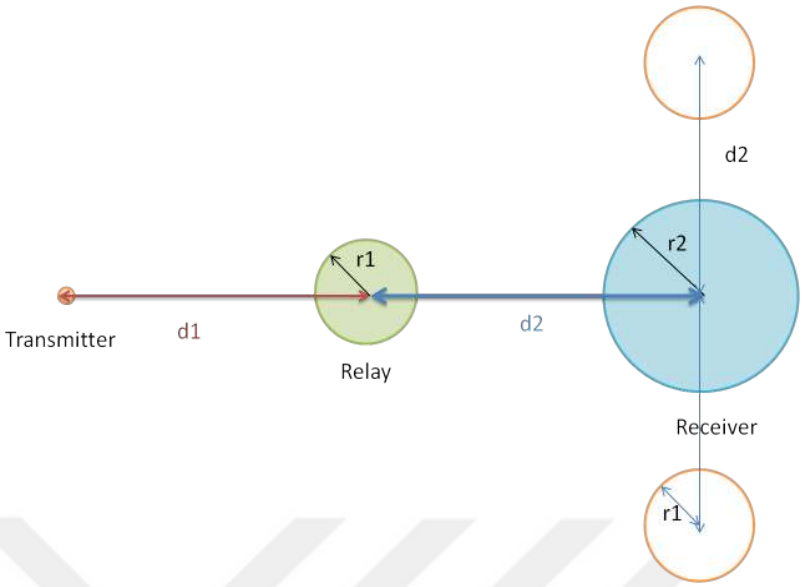

Figure 4.11: Illustration of the three relays system.

seen, the signal is strongly amplified, at the cost of a communication delay.

4.5 Three Relays Tentative Scenario

Due to the promising results of the aforementioned optimal relay topology, a tentative scheme consisting of three relays is shortly investigated. An illustration for this scheme is provided in Figure 4.11, where the three relays (green and white nodes) are identical, and they are placed at same distances with respect to the Rx (the blue node), and the molecules are again assumed to be emitted from a point Tx. Following a similar idea to the case with only one relay, the three relays will collect molecules until some specified time and then direct them towards the Rx, from their respective closest points to it. Let the green relay be denoted as Rel_1, the top white relay as Rel_2 and the down one as Rel_3. As it can be expected, the molecules received from Rel_2 and Rel_3 are much less compared to Rel_1. For this reason, it is proposed that Rel_1 emits its collected molecules without any amplification, whereas Rel_2 and Rel_3 will amplify the number of molecules collected. It is noteworthy to mention that due to symmetry, the signals arriving at Rel_2 and Rel_3 are expected to be very similar, thus same amplification factor (α) can be used.

As this is only a tentative study inspired by the optimal relay work, the parameters given in Table 4.2 are not optimized. To this point, the potential improvement

Table 4.2: The parameters used for the three relays scheme simulation.

Parameter	Value
r_1	1 μm
r_2	4.5 μm
d_1	3 μm
d_2	7 μm
T_s	0.25 s
D	79.4 $\mu m^2/s$
τ	0.12 s
N	10^5
α	600

by using more relay nodes is to be investigated, thus tentative results for these parameters are shown below. As it can be seen from Figure 4.12, the signals arriving from the relays at the Rx node are very similar to each other. There is a huge improvement in the received signal shape for the three relays case, as shown in Figure 4.13, which comes at the cost of a longer delay and requirement for more transmitted molecules due to the signal amplification. In Figure 4.14, it is clear that the BER performance is also enhanced. Future works may focus on optimizing this system in terms of α, τ and T_s values.

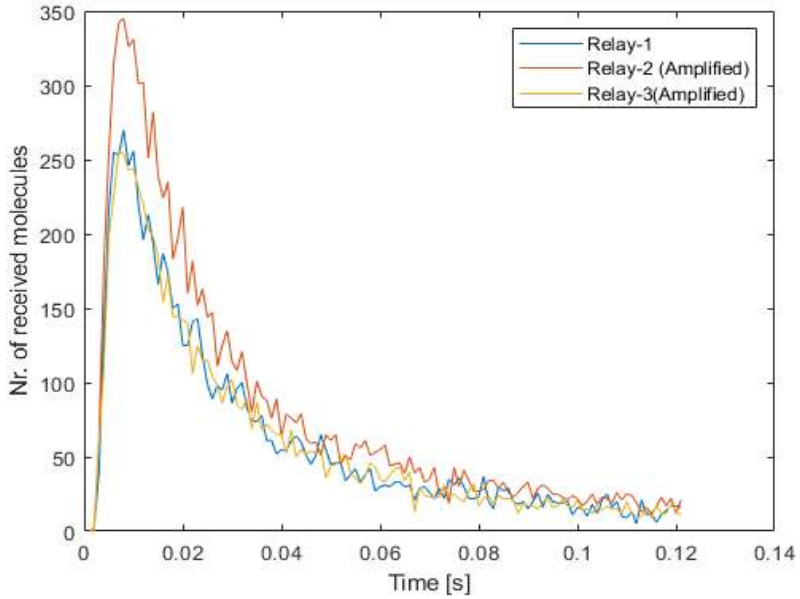

Figure 4.12: Number of molecules received in the Rx from each relay.

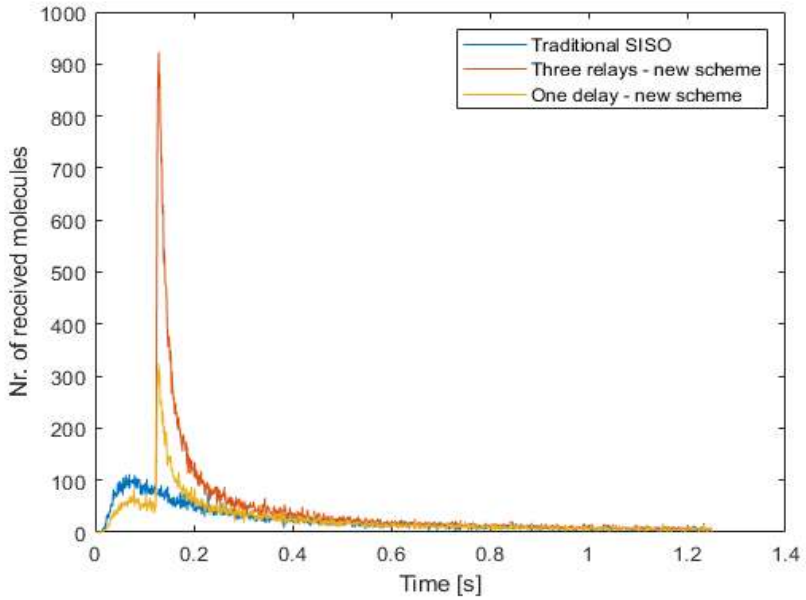

Figure 4.13: Comparison of the hitting rate of molecules for the three relays scheme and conventional SISO scheme.

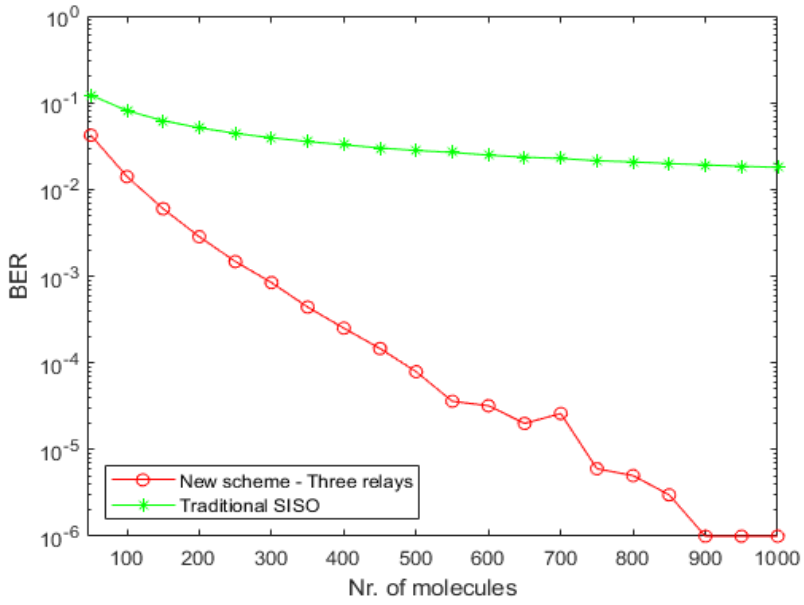

Figure 4.14: Comparison of BER between the three relays scheme and the conventional SISO setting.

Chapter 5

MOLECULAR BEAMFORMING FOR ACTUATION IN MOLECULAR COMMUNICATION NETWORKS

5.1 Motivation

Nano communication offers a vast set of prospective applications in fields such as medicine and healthcare. As stated in [Abbasi et al., 2016], nano communication technologies enable noninvasive solutions for reaching remote and delicate human body parts, which can clearly enhance the processes of diagnosis and treatment of various health related issues. One of the advantages of using MC for medical therapies is its capability to prevent side effects on human health [Cevallos et al., 2019]. A number of applications have been proposed in the literature, starting from disease detection [Felicetti et al., 2014] to disease treatment by using targeted drug delivery [Chahibi et al., 2013], immune system triggering [Chude-Okonkwo et al., 2019], nanosurgery [Felicetti et al., 2016], etc.. For example, a discussion about the treatment of diabetes by means of nanotechnology is given in [DiSanto et al., 2015]. Recent studies propose that the level of glucose can be constantly measured by means of *in vivo* sensors, and responses to changes in its level can be made possible through novel advancements in insulin delivery systems. A conceptual mechanism is developed in [El-Hajj and Chahine, 2021], where MC is used for the signalling needed to initiate the insulin pump.

Small scale communication is highly related to the progression and development of sensors. Sensors play a crucial role in collecting data, which is essential for monitoring and analysing a specific environment. For instance, the authors of [Felicetti et al., 2014] propose a network that may be used to detect circulating tumoral cells, which basically relies on mobile sensors that store information whenever a tumor cell is encountered in the blood circulatory system. In [Shitharth et al., 2021], the

authors analyze the impact of the integration of nano senors with big data and the benefits that follow when applied to healthcare applications. Clearly, the sensing accuracy of these sensors is a very decisive parameter, especially when used for applications related to human health. There are parameters and regulations in the literature for measuring the accuracy of nano sensors. For example, evaluation of glucose biosensors in terms of spectral response, linearity, sensitivity, limit of detection, kinetic response, reversibility, stability, precision, and accuracy is proposed in [Aloraefy et al., 2014]. This study evaluates its results in accordance with the regulations given in [for Standardization, 2003]. Similarly, the authors of [Aberer et al., 2020] investigated the accuracy and stability of a biosensor used to monitor arterial glucose. As expected, sensing errors are quite possible in real-time applications. Attempts to increase the accuracy of nano systems can be made in terms of nano sensors design and system implementation.

There are several works in the literature focusing on cooperative sensing for improving the accuracy when the sensors are imperfect. For example, the authors of [Khaloopour et al., 2020] and [Khaloopour et al., 2021] focus on both abnormality detection and abnormality localization in fluidic mediums, achieved by cooperative activation of several mobile sensors. They conclude that the detection performance enhances due to the collaboration between the sensors for activating each other. The authors of [Mosayebi et al., 2018] propose target detection via several sensors distributed in a tissue. When a target is present and encountered by these sensors, they get activated and react in notifying about the presence of the target. The authors of [Varshney et al., 2018b] focus on abnormality detection by several cooperative nanomachines, where the final decision is made by applying OR and AND logic-based fusion rules.

Parallel to the advancements in RF communication systems, novel designs on the small scale levels have been proposed in order to overcome challenges that are faced by these systems and enhance their performance. For instance, authors of [Koo et al., 2016] propose several detection algorithms for a MIMO MC design and they implement these algorithms on a testbed for real-time evaluation. Their analysis is based on the consideration ILI and ISI for the MIMO design, which are the two of

the main challenges faced by MCvD systems. IM based transmission for MCvD systems is introduced in [Gursoy et al., 2019b], where several modulation schemes are proposed for the mitigation of ISI and ILI. Space-time equalization algorithms are then introduced for further combating ISI and ILI, leading to significant improvement in the performance of MIMO systems and low detection complexity [Gursoy et al., 2020].

Inspired by such RF communication systems, a novel molecular beamforming scheme that aims to improve the actuation accuracy in MC networks is proposed. From a signal processing perspective, beamforming is defined as a technique used for *directing* a signal towards a particular receiving node [Van Veen and Buckley, 1988]. The main benefit of beamforming in RF is the enhancement of the network performance by boosting the signal quality in the intended direction. This is achieved by appropriately delaying transmitted signal components.

Similar to this concept, the proposed idea for MC is based on the superposition of delayed signal components such that a stronger overall signal is received at the Rx node. This topology can find application in improving the actuation accuracy of MC networks, for which, as mentioned above, sensing errors are probable. Let us assume that several sensors have to monitor and stabilize the sugar level of a patient with diabetes. According to the collected information, the duty of these sensors is to initialize a request for an insulin pump when deemed necessary. The main motivation behind this study relies on the idea that as individual sensors are prone to sensing errors, a network which consists of a larger number of sensors will result in having an overall higher accuracy level. From a communication system's perspective, a scheme incorporating several sensors and two spherical Rx nodes, the actuators (the proposed idea can be easily extended to more than two Rxs) is examined. These sensors are transmit nodes which emit molecules in accordance with the information that they have, with the purpose of activating one Rx at a time, i.e., they will collectively try to activate one actuator or the other one. A sensing error in the aforementioned scenario could be that the sensors do not activate the node that holds the insulin, when needed. It is claimed that, given that each sensor senses incorrectly with a probability of error p, the actuation error rate of the

overall system decreases if the number of utilized sensors is increased. Molecular beamforming is introduced such that signal components sent from different sensors are delayed and their respective signal strengths are adjusted (by controlling the number of emitted molecules from each node), in order for the received signal to be strong enough and decoded with minimum error probability.

In order to validate the proposed system, an analytical approach is followed for demonstrating the impact on the actuation accuracy. Two different error sources are introduced, which are referred to as the activation and deactivation errors. The former occurs when the intended Rx node is not activated and the latter results from the activation of the non-intended Rx node. Three different scenarios are studied; the first and second scenarios examine the impact of molecular beamforming on the activation error only and the third one takes into consideration both error sources, which is represented as the composite error case. For the two first scenarios, the error rate when there is a pre-defined threshold on the Rx nodes is examined, and then it is assumed that these nodes can communicate with each other to decide which one of them will be activated. As expected, the second scenario can achieve a better performance, which comes at the cost of increased system complexity due to the need for coordination among the two actuators.

The main contributions of this work are:

- The design of a novel system inspired by beamforming used for actuation in MC networks,
- Analysis of the topology for which the Txs form a ULA for understanding the impact of the proposed system in terms of actuation accuracy,
- Analysis of a random topology for providing insight into a more practical scenario,
- Presentation of analytical and simulation results for the actuation error probability.

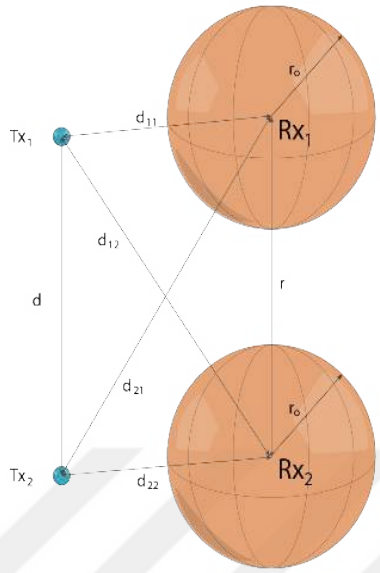

Figure 5.1: The proposed ULA system that consists of two Txs (blue spheres) and two Rxs (orange spheres).

The system model, actuation accuracy derivation and the obtained results are presented in the following sections.

5.2 System Model

In this section, the proposed system model is presented. As aforementioned, the proposed system consists of several transmitting sensors and two receiving actuator nodes. The topology in which the Txs form a ULA is firstly introduced, and then a more realistic one is presented, where the Txs/sensors are randomly located. Throughout this study, some key design characteristics are followed, which are introduced in this section.

5.2.1 ULA Topology

Figure 5.1 illustrates the topology that is introduced in this section. As in the majority of analytical works in the MC literature, it is assumed that the Txs are

point ones. The blue spheres are two point Txs, and the orange spheres are two spherical Rxs with equal radii r_o. The distances between the transmitting and the centers of the receiving nodes are denoted by d_{ij}, where i stands for the Tx and j for the Rx index, respectively. In this case, there are two of each type of nodes and due to symmetry, $d_{11} = d_{22}$ and $d_{12} = d_{21}$. The main idea is that it is preferred to have one of the Rxs/actuators to be active at a time, and it is the Txs' task to emit molecules such that they achieve this. In the literature, the SISO topology of an MCvD system is well-studied and the analytical basis of the channel characteristics for a point Tx and absorbing spherical Rx is given in Chapter 2. However, in the proposed scenario, each emission from a Tx constitutes a SIMO topology. The analytical foundation for this case is given in [Yaylali et al., 2021], as mentioned before, and the approximations provided by this study will come of use for the proposed actuation error rate modelling.

As seen from Figure 5.1, Tx 1 (Tx_1) is closer to Rx 1 (Rx_1), so the signal transmitted from this node is indeed stronger compared to that arriving from Tx 2 (Tx_2) to Rx_1. In other words, it is expected that if both Txs are emitting the same number of molecules, then Rx_1 will receive a bigger fraction from Tx_1 than Tx_2. As a result, if Rx_1 is the intended Rx to be activated and Tx_2 is emitting, a large fraction of molecules transmitted by Tx_2 will arrive at Rx_2. In the case where a Rx is activated if the number of received molecules exceeds a threshold, this would cause an actuation error. Even if less power is allocated to the further Tx, its contribution will not be effective since the further Tx contributes more molecules to the non-intended Rx. For this reason, it is decided to allow the Txs to emit only when their effect is constructive to the intended Rx, not to the other one. Basically, for the topology shown in Figure 5.1, Tx_1 will only emit when Rx_1 is the intended Rx to be activated. On the other hand, the second Tx will only emit when Rx_2 is the intended Rx.

The actuation decision at the Rx side is done based on a comparison between the number of received molecules and a threshold value. To this end, it is proposed to count the molecules received over an interval of length τ around the signal's peak, $[t_p - \frac{\tau}{2}, t_p + \frac{\tau}{2}]$, where t_p is the peak time. Let the number of molecules around

the peak of the signal received at Rx_j be denoted by $N_{Rx_j}[t_p-\frac{\tau}{2}, t_p+\frac{\tau}{2}]$. Assuming that Rx_1 is to be activated and that both Txs are sensing correctly, the received signal would consist of one component only, the signal transmitted from Tx_1. In other words, if the messages from both Txs are annotated as m_1 and m_2, the ideal case for activating Rx_1 would be $(m_1,m_2) = (1, 0)$, where m_i corresponds to the case where Tx_i transmits molecules. Due to the sensing error, the Txs may try to actuate incorrect Rxs. The conditional probability table for the four possible cases, $P\big(N_{Rx_1}[t_p-\frac{\tau}{2}, t_p+\frac{\tau}{2}](m_1, m_2)|A = 1\big)$, where $N_{Rx_1}[t_p-\frac{\tau}{2}, t_p+\frac{\tau}{2}](m_1, m_2)$ stands for the number of received molecules around the peak depending on the emissions from the Txs and $A=1$ denotes the event that Rx_1 is to be activated, is given in Table 5.1. The sensing error probability is denoted by p. The table is only shown for $N_{Rx_1}[t_p-\frac{\tau}{2}, t_p+\frac{\tau}{2}]$, but a similar logic can be followed for $N_{Rx_2}[t_p-\frac{\tau}{2}, t_p+\frac{\tau}{2}]$ as well.

Table 5.1: Probability table for the topology with two Txs.

(m_1, m_2)	Probability
$(1, 0)$	$(1-p)^2$
$(0, 1)$	p^2
$(1, 1)$	$p(1-p)$
$(0, 0)$	$p(1-p)$

Up to this point, the system consisting of two Txs has been discussed. This case is trivial, and the cases when the number of Txs is increased should be actually considered. Figure 5.2 illustrates the proposed system consisting of twelve point Txs forming a ULA, while keeping d from Tx_1 to Tx_{12} unchanged, and two spherical Rxs, as before. In this case, if Rx_1 is to be activated, the transmit nodes from Tx_1 to Tx_6 are ideally turned on and the rest are off; so the overall received signal consists of six components. Since the peaks of these component signals occur at different times, it is proposed that the emissions are delayed such that their peaks almost overlap at the Rx node. To do so, the peak time of each component can be calculated beforehand and the delay times can be arranged in such a way that

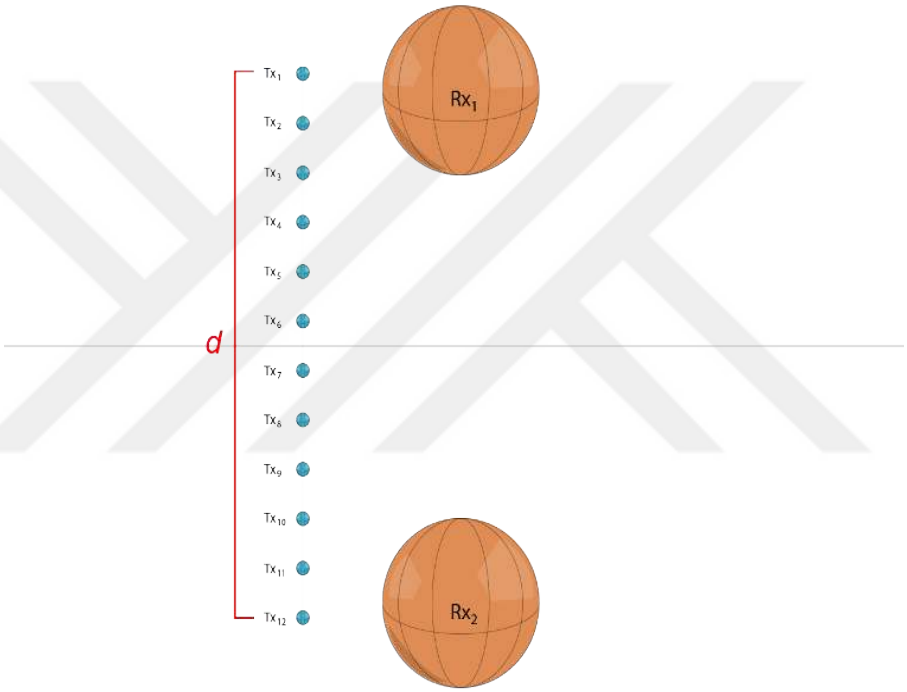

Figure 5.2: The proposed ULA system that consists of twelve Txs (blue spheres) and two Rxs (orange spheres).

each component signal's peak overlaps with the latest peak that occurs among the component signals.

Moreover, since these Txs may be on/off due to a sensing error, it is only fair to allow them to contribute the same level to the received signal. If not, a Tx with a strong communication channel can easily cause an actuation error if it senses incorrectly. In order to realize this, a power normalization technique is proposed, which corresponds to arranging the number of emitted molecules from each Tx in advance. This is performed by computing the area under the PDF-like curves of each component for τ seconds around the peak, and adjusting the number of emitted molecules such that all the computed integrals for an activation are equal to each other. The PDF-like curves of each of the component signals are obtained as given in [Yaylali et al., 2021].

To sum up, several key design characteristics are proposed in order to be able to benefit from molecular beamforming in actuation accuracy in MC networks. First of all, the Txs are ideally on or off, depending on their contribution towards the actuation of the receiving nodes. Secondly, Txs emit with some pre-defined delay time, in order for the signal components to arrive almost simultaneously at the Rx side, such that an overall stronger signal is received. Lastly, power normalization is performed before emission by adjusting the number of emitted molecules from each Tx such that they contribute the same fraction of molecules around the peak of the overall received signal. In the following sections, the actuation error rate is computed for the ULA topology with $2K$ Txs, where $K = 1, 2, 3, 4, 5$, and it is shown that as K increases, so does the actuation accuracy. In Figure 5.2, an hypothetical line which passes from $\frac{d}{2}$ is drawn in order to illustrate which Txs will be on for each activation. The coordinates of the nanomachines used in this study for $K = 1$ are given in Table 5.2.

As for the cases when $K > 1$, the coordinates can be easily computed knowing that d is kept unchanged and the Txs are equally spaced. The roughly estimated peak times, areas under the PDF-like curves and adjusted number of molecules emitted from each Tx are shown in Table 5.3 for $K = 2$ as an illustration of the explained design steps.

Table 5.2: The coordinates of the nanomachines of Figure 5.1

Nanomachine	Coordinates
Rx_1	[0,0,10] μm
Rx_2	[0,0,-10] μm
r_o	5 μm
Tx_1	[10,0,10.5] μm
Tx_2	[10,0,-10.5] μm

Table 5.3: The estimated parameters of the ULA topology with $K=2$ Txs.

Tx_i	t_{p_1}	t_{p_2}	I_1	I_2	M_{Rx_1}	M_{Rx_2}	ϕ_1	ϕ_2
Tx_1	$0.055s$	$0.55s$	0.095	0.003	$1.05e4$	–	$0.495s$	$0s$
Tx_2	$0.1s$	$0.295s$	0.053	0.0137	$1.9e4$	–	$0.45s$	$0.255s$
Tx_3	$0.295s$	$0.1s$	0.0137	0.053	–	$1.9e4$	$0.255s$	$0.45s$
Tx_4	$0.55s$	$0.055s$	0.003	0.095	–	$1.05e4$	$0s$	$0.495s$

In Table 5.3, t_{p_1} and t_{p_2} are the estimated peak times of the signals received from Tx_i at Rx_1 and Rx_2 respectively. Afterwards, the area under the PDF-like curves for τ seconds around these peaks are computed, given as I_1 and I_2. An example of I_1 computation for the signal arriving at Rx_1 from Tx_1 is shown in Figure 5.3. The shaded area corresponds to the fraction of received molecules during the $[t_p - \frac{\tau}{2}, t_p + \frac{\tau}{2}]$ interval. Referring to Table 5.3, Tx_1 is clearly in favor of Rx_1, thus it will be emitting when Rx_1 is to be activated and it will be turned off for the actuation of Rx_2. As explained above, the number of emitting molecules is adjusted such that each "on" Tx contributes the same amount of molecules to the overall received signal, given as M_{Rx_1} and M_{Rx_2} in the table. In this study, each Tx is contributing 1000 molecules around the peak. In other words, the value of I_1 for the component shown in Figure 5.3 when Tx_1 is emitting $M_{Rx_1} = 1.05e4$ molecules is 1000. Moreover, the peak times are different for each signal, as expected. The delay times of each

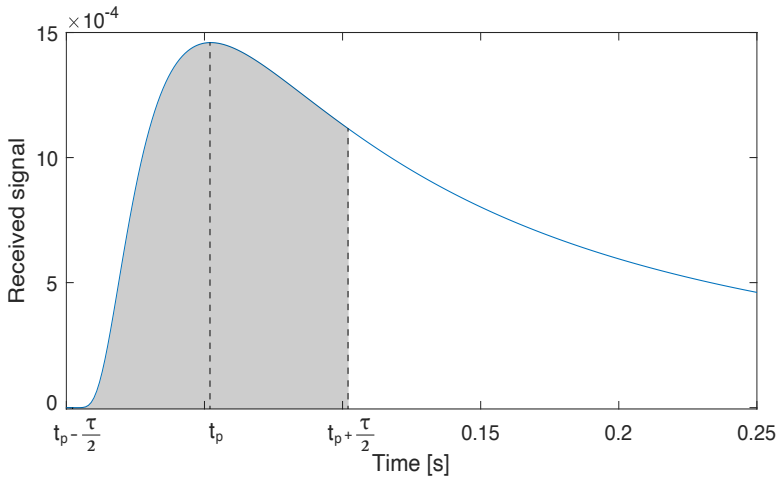

Figure 5.3: Computation of I_1 for the signal received at Rx_1 when Tx_1 is emitting of the ULA topology with $K = 2$ Txs.

emission are computed based on these peak times, denoted by ϕ_1 and ϕ_2 in Table 5.3 for the activation of Rx_1 and Rx_2, respectively. For the activation of Rx_1, the peak occurring last is that of the emission from Tx_4, thus all the other Txs, when emitting, emit with $\phi_1 = 0.55 - t_{p_1}$ seconds delay. The symmetry of the ULA cases is also clearly shown by this table.

These steps are illustrated in Figure 5.4 for the activation of Rx_1 for the ULA topology of $K = 2$ Txs. Due to symmetry, the same idea would follow for the activation of Rx_2. In Figure 5.4a, the signal components at their respective peak times are shown, where component 1 refers to the one arriving from Tx_1 and so on. The computation of ϕ_1 is done with respect to the peak occurring the last (4^{th} component). In Figure 5.4b, the overall signal components are shown, as if all Txs were emitting at $t = 0$. The total received signal when all these components' peaks are overlapping is shown in Figure 5.4c.

5.2.2 Random Topology

The ULA case is considered in this work to simplify the concept behind the proposed method. However, Txs forming a perfect ULA may not be feasible in real life applications. For this reason, a random topology is also presented, such that the

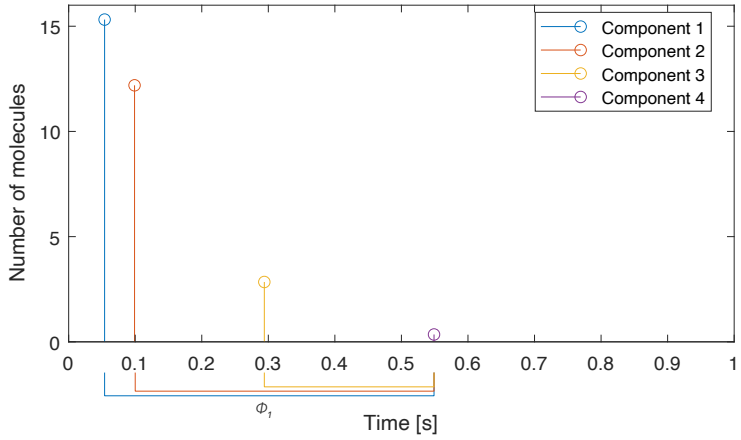

(a)

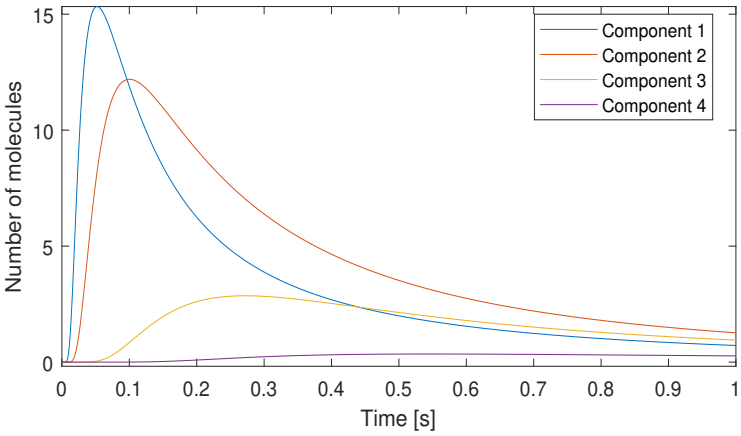

(b)

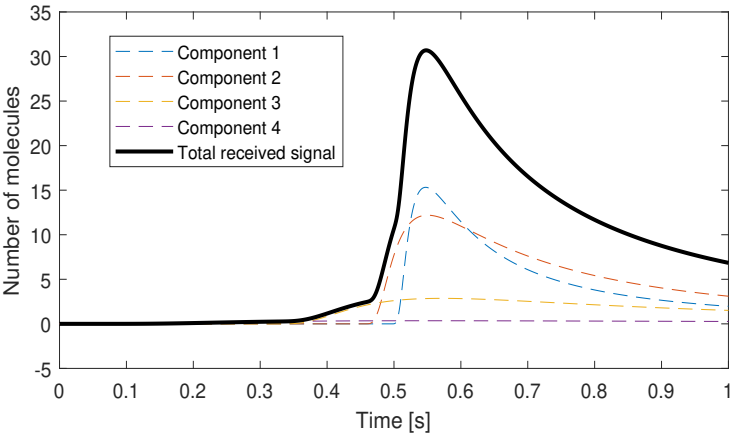

(c)

Figure 5.4: ULA topology of $K = 2$ Txs: (a) The four signal components at their respective peak times. (b) The overall received signal components, assuming that all Txs emit at $t = 0s$. (c) The total received signal when all Txs emit at their respective times according to ϕ_1.

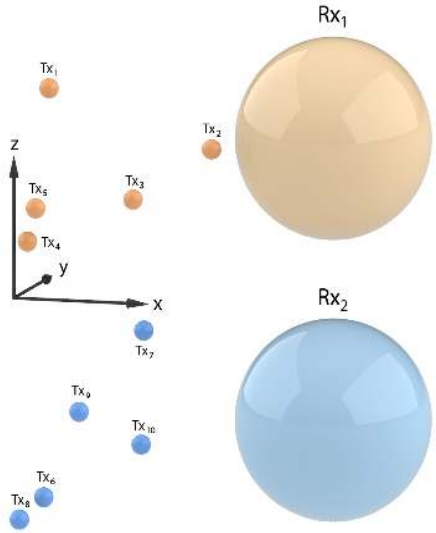

Figure 5.5: The random system that consists of ten Txs and two Rxs.

Txs are uniformly and randomly distributed inside a 3-D cuboid, with boundaries ranging from [-10 μm, 10 μm]. A randomly generated set of coordinates for the $K=5$ case is given in Table 5.4, such that Tx_1 to Tx_5 are to be on for the activation of Rx_1, whereas the rest for the activation of Rx_2. The corresponding system is presented in Figure 5.5. In the following sections, the analytical modelling of the actuation accuracy for different scenarios is given, followed by a comparison between theoretical and simulation-based results.

5.3 Actuation Accuracy

In this section, three different scenarios for analyzing the actuation accuracy are presented. The proposed scheme may be used in different applications, thus the actuation accuracy may be related to two different kind of error sources, defined as the activation and deactivation errors. The first one is related to the error occurring as a result of the intended Rx not being activated, whereas the second occurs when the non-intended Rx is mistakenly activated. The impact of molecular beamforming on the activation error is investigated for two different scenarios. In the first sce-

Table 5.4: The coordinates of the nanomachines of the random topology.

Nanomachine	Coordinates
Rx_1	[14,10,7] μm
Rx_2	[14,10,-7] μm
r_o	5 μm
Tx_1	[1,3,10] μm
Tx_2	[9,5,7] μm
Tx_3	[6,1,5] μm
Tx_4	[1,-1,3] μm
Tx_5	[2,-3,5] μm
Tx_6	[3,-5,-9] μm
Tx_7	[4,10,-3] μm
Tx_8	[2,-6,-10] μm
Tx_9	[6,-9,-4] μm
Tx_{10}	[5,6,-8] μm

nario, Rxs compare the number of molecules received around their individual peaks with a predefined threshold value, which if exceeded, makes the Rx active. In the second scenario, the Rxs are assumed to be able to cooperate. They compare their received number of molecules and the Rx that has received the larger number of molecules gets actuated. At last, both activation and deactivation errors are examined simultaneously. The analytical formulations for calculating the actuation error are derived for each of the aforementioned cases.

5.3.1 Predefined Thresholding: Activation Error

The derivation of the activation error rate with predefined threshold values is given for the topology shown in Figure 5.1, the two Txs case. The same idea is followed for the cases when $K > 1$. The fraction of the molecules emitted from Tx i and received by Rx j, F_{hit}^{ij} is computed following the approximations given in [Yaylali

et al., 2021], given as

$$F_{hit}^{11}(t_d) \cong \frac{r_{o_1}}{d_{11}}\text{erfc}\left(\frac{d_{11}-r_{o_1}}{\sqrt{4\,D\,t_d}}\right) - \frac{r_{o_2}}{d_{12}}\text{erfc}\left(\frac{d_{12}-r_{o_2}}{\sqrt{4\,D\,t_d}}\right) * \frac{r_{o_1}}{r_{v12}}\text{erfc}\left(\frac{r_{v12}-r_{o_1}}{\sqrt{4\,D\,t_d}}\right), \quad (5.1)$$

$$F_{hit}^{21}(t) \cong \frac{r_{o_1}}{d_{21}}\text{erfc}\left(\frac{d_{21}-r_{o_1}}{\sqrt{4\,D\,t}}\right) - \frac{r_{o_2}}{d_{22}}\text{erfc}\left(\frac{d_{22}-r_{o_2}}{\sqrt{4\,D\,t}}\right) * \frac{r_{o_1}}{r_{v22}}\text{erfc}\left(\frac{r_{v22}-r_{o_1}}{\sqrt{4\,D\,t}}\right), \quad (5.2)$$

$$F_{hit}^{12}(t) \cong \frac{r_{o_2}}{d_{12}}\text{erfc}\left(\frac{d_{12}-r_{o_2}}{\sqrt{4\,D\,t}}\right) - \frac{r_{o_1}}{d_{11}}\text{erfc}\left(\frac{d_{11}-r_{o_1}}{\sqrt{4\,D\,t}}\right) * \frac{r_{o_2}}{r_{v11}}\text{erfc}\left(\frac{r_{v11}-r_{o_2}}{\sqrt{4\,D\,t}}\right), \quad (5.3)$$

$$F_{hit}^{22}(t_d) \cong \frac{r_{o_2}}{d_{22}}\text{erfc}\left(\frac{d_{22}-r_{o_2}}{\sqrt{4\,D\,t_d}}\right) - \frac{r_{o_1}}{d_{21}}\text{erfc}\left(\frac{d_{21}-r_{o_1}}{\sqrt{4\,D\,t_d}}\right) * \frac{r_{o_2}}{r_{v21}}\text{erfc}\left(\frac{r_{v21}-r_{o_2}}{\sqrt{4\,D\,t_d}}\right), \quad (5.4)$$

where r_{vij} denotes the virtual release point from the $i-th$ Tx to the $j-th$ Rx and D is the diffusion coefficient that depends on the utilized fluid environment and the properties of the molecules. As discussed earlier, the Txs emit with some delay in order for these component signals to arrive almost simultaneously at the Rx side. By observing the peaks of the separate components, the delay is computed such that each component arrives in accordance with the one whose peak occurs the last. As a result, the time is indexed differently for $F_{hit}^{11}(t_d)$ and $F_{hit}^{22}(t_d)$, showing that these components are delayed. The expected number of molecules around the peak of Rx_1 can be computed as a function of m_1 and m_2, as shown below

$$\begin{aligned} E\big[N_{Rx_1}[t_p-\frac{\tau}{2},t_p+\frac{\tau}{2}](m_1,m_2)\big] \cong & m_1 \times M_{Tx} \times \Big(F_{hit}^{11}(t_p+\frac{\tau}{2}) - F_{hit}^{11}(t_p-\frac{\tau}{2})\Big) + \\ & m_2 \times M_{Tx} \times \Big(F_{hit}^{21}(t_p+\frac{\tau}{2}) - F_{hit}^{21}(t_p-\frac{\tau}{2})\Big), \end{aligned} \quad (5.5)$$

where M_{Tx} is the number of molecules emitted from each Tx. Due to the symmetry of this topology, if on, each Tx emits the same number of molecules. As an example, the expected number of molecules around the peak of the signal received in Rx_1 for the ideal case is

$$E[N_{Rx_1}[t_p-\frac{\tau}{2},t_p+\frac{\tau}{2}](1,0)] \cong M_{Tx} \times \Big(F_{hit}^{11}(t_p+\frac{\tau}{2}) - F_{hit}^{11}(t_p-\frac{\tau}{2})\Big), \quad (5.6)$$

which helps in modeling $N_{Rx_1}[t_p-\frac{\tau}{2},t_p+\frac{\tau}{2}]$ as

$$N_{Rx_1}[t_p-\frac{\tau}{2},t_p+\frac{\tau}{2}](1,0) \sim B(M_{Tx}, p_{peak,\tau}^{11}). \quad (5.7)$$

Each molecule arrives at the Rx around the signal's peak with a probability of $p^{11}_{peak,\tau} = \left(F^{11}_{hit}(t_p+\frac{\tau}{2}) - F^{11}_{hit}(t_p-\frac{\tau}{2})\right)$. Here, $p^{11}_{peak,\tau}$ is the success probability of the Binomial distribution with M_{Tx} trials, given that the Txs are emitting M_{Tx} molecules. Then, as proposed in [Yilmaz et al., 2015], the Gaussian approximation can be used to model (6) as

$$N_{Rx_1}[t_p-\frac{\tau}{2}, t_p+\frac{\tau}{2}](1,0) \sim \mathcal{N}\left(M_{Tx}\times p^{11}_{peak,\tau}; M_{Tx}\times p^{11}_{peak,\tau}\times(1-p^{11}_{peak,\tau})\right). \quad (5.8)$$

The same idea is followed for the other three cases as well. Knowing that an error occurs when the number of received molecules is smaller that the predefined threshold values, the probability of error can be computed as

$$\begin{aligned} P(err) = P\left(N_{Rx_1}[t_p-\frac{\tau}{2}, t_p+\frac{\tau}{2}](m_1,m_2) < \gamma_1 | A=1\right)\times P(A=1) + \\ P\left(N_{Rx_2}[t_p-\frac{\tau}{2}, t_p+\frac{\tau}{2}](m_1,m_2) < \gamma_2 | A=2\right)\times P(A=2), \end{aligned} \quad (5.9)$$

where γ_1 and γ_2 are the predefined thresholds, which are equal due to the symmetry of the scheme, thus $\gamma_1 = \gamma_2 = \gamma$. Moreover, $P(A=1) = P(A=2) = \frac{1}{2}$ in the simulations, resulting in

$$\begin{aligned} P(err) = \frac{1}{2}\Big[P\left(N_{Rx_1}[t_p-\frac{\tau}{2}, t_p+\frac{\tau}{2}](m_1,m_2) < \gamma | A=1\right) + \\ P\left(N_{Rx_2}[t_p-\frac{\tau}{2}, t_p+\frac{\tau}{2}](m_1,m_2) < \gamma | A=2\right)\Big]. \end{aligned} \quad (5.10)$$

The components in (10) are equal to each other, so the probability of error can be finally expressed as

$$P(err) = P\left(N_{Rx_1}[t_p-\frac{\tau}{2}, t_p+\frac{\tau}{2}](m_1,m_2) < \gamma | A=1\right). \quad (5.11)$$

From the Gaussian approximations above, the probability of error by using the $Q(.)$ function can be computed in the form

$$P\left(\ N_{Rx_1}[t_p-\frac{\tau}{2}, t_p+\frac{\tau}{2}](1,0) < \gamma | A=1\ \right) = (1-p)^2 \times Q\left(\frac{M_{Tx}\times p^{11}_{peak,\tau} - \gamma}{\sqrt{M_{Tx}\times p^{11}_{peak,\tau}\times(1-p^{11}_{peak,\tau})}}\right). \quad (5.12)$$

Then, the probability of error is analytically computed by summing up the error as a result of the four cases. The same process is followed for the cases of $K>1$.

5.3.2 Mutual Thresholding: Activation Error

Unlike the predefined thresholding case, the decision whether a Rx is active or not is done based on the comparison of the number of molecules absorbed in the peak window between the two Rxs. As expected, the complexity is increased for this scenario, since it requires a communication channel between the two receiving nodes. Following a similar approach as before, the error probability for the two Txs case can be computed by

$$P(err) = P\left(N_{Rx_1}[t_p - \frac{\tau}{2}, t_p + \frac{\tau}{2}](m_1, m_2) < N_{Rx_2}[t_p - \frac{\tau}{2}, t_p + \frac{\tau}{2}](m_1, m_2) | A = 1\right), \tag{5.13}$$

Since the receptions on the Rxs are independent from each other, the distribution of $N_{Rx_1}[t_p - \frac{\tau}{2}, t_p + \frac{\tau}{2}](m_1, m_2) - N_{Rx_2}[t_p - \frac{\tau}{2}, t_p + \frac{\tau}{2}](m_1, m_2)$ random variable can be given as follows

$$\begin{aligned} &N_{Rx_1}[t_p - \frac{\tau}{2}, t_p + \frac{\tau}{2}](m_1, m_2) - N_{Rx_2}[t_p - \frac{\tau}{2}, t_p + \frac{\tau}{2}](m_1, m_2) \sim \\ &\mathcal{N}\left(\frac{\mu_{N_{Rx_1}[t_p - \frac{\tau}{2}, t_p + \frac{\tau}{2}](m_1, m_2)} - \mu_{N_{Rx_2}[t_p - \frac{\tau}{2}, t_p + \frac{\tau}{2}](m_1, m_2)}}{\sqrt{\sigma^2_{N_{Rx_1}[t_p - \frac{\tau}{2}, t_p + \frac{\tau}{2}](m_1, m_2)} + \sigma^2_{N_{Rx_2}[t_p - \frac{\tau}{2}, t_p + \frac{\tau}{2}](m_1, m_2)}}}\right), \end{aligned} \tag{5.14}$$

where $\mu_{N_{Rx_1}[t_p - \frac{\tau}{2}, t_p + \frac{\tau}{2}](m_1, m_2)}$ and $\mu_{N_{Rx_2}[t_p - \frac{\tau}{2}, t_p + \frac{\tau}{2}](m_1, m_2)}$ are the respective means of $N_{Rx_1}[t_p - \frac{\tau}{2}, t_p + \frac{\tau}{2}]$ and $N_{Rx_2}[t_p - \frac{\tau}{2}, t_p + \frac{\tau}{2}]$, whereas $\sigma^2_{N_{Rx_1}[t_p - \frac{\tau}{2}, t_p + \frac{\tau}{2}](m_1, m_2)}$ and $\sigma^2_{N_{Rx_2}[t_p - \frac{\tau}{2}, t_p + \frac{\tau}{2}](m_1, m_2)}$ are their variances, respectively. The activation error can then be analytically computed.

5.3.3 Composite Error

In the aforementioned cases, no error is encountered as long as the intended Rx is activated. However, in some applications, the system designer may want to make sure that only the intended Rx must be active. In this case, when both Rxs are active given that only one is intended may count towards an error. Therefore, it can be considered that the total error to consist of both activation and deactivation error sources and call this case the composite error case. The probability of correct

actuation is given as

$$P(c) = \frac{1}{2}\Big[P\left(N_{Rx_1}[t_p-\frac{\tau}{2},t_p+\frac{\tau}{2}](m_1,m_2)>\gamma \wedge N_{Rx_2}[t_p-\frac{\tau}{2},t_p+\frac{\tau}{2}](m_1,m_2)<\gamma|A=1\right)+ P\left(N_{Rx_2}[t_p-\frac{\tau}{2},t_p+\frac{\tau}{2}](m_1,m_2)>\gamma \wedge N_{Rx_1}[t_p-\frac{\tau}{2},t_p+\frac{\tau}{2}](m_1,m_2)<\gamma|A=2\right)\Big]. \tag{5.15}$$

Due to the symmetry of the scheme and the independence of the two reception events, the error probability can then be computed as

$$P(err)=1-P\left(N_{Rx_1}[t_p-\frac{\tau}{2},t_p+\frac{\tau}{2}](m_1,m_2)>\gamma|A=1\right)\times P\left(N_{Rx_2}[t_p-\frac{\tau}{2},t_p+\frac{\tau}{2}](m_1,m_2)<\gamma|A=1\right). \tag{5.16}$$

As an example, shown for the (m_1,m_2)=$(1,0)$, the error probability can be computed as

$$P\left(\ N_{Rx_1}[t_p-\frac{\tau}{2},t_p+\frac{\tau}{2}](1,0)<\gamma|A=1\ \right)\times P\left(\ N_{Rx_2}[t_p-\frac{\tau}{2},t_p+\frac{\tau}{2}](1,0)>\gamma|A=1\ \right)= (1-p)^2\times Q\left(\frac{\gamma-\mu_{Rx_{1_{peak}}(1,0)}}{\sigma_{N_{Rx_1}[t_p-\frac{\tau}{2},t_p+\frac{\tau}{2}](1,0)}}\right)\times Q\left(\frac{\mu_{Rx_{2_{peak}}(1,0)}-\gamma}{\sigma_{N_{Rx_2}[t_p-\frac{\tau}{2},t_p+\frac{\tau}{2}](1,0)}}\right). \tag{5.17}$$

The threshold value γ can be optimized for this case, such that the probability of error reaches a minimum. The overall results of the predefined thresholding, mutual thresholding and the composite error case are presented in the following section.

5.4 Simulation Results

The validation of the proposed scheme is done by comparing the analytical results following the derivations done in Section III with the results obtained from computer simulations. The Txs are assumed to correctly sense for 95% of the time, such that $p=0.05$. The peak times of the received signal components are roughly estimated from their PDF-like curves. The window size around the peak is selected as $\tau = 0.1s$. As for the power normalization procedure previously explained, the number of molecules emitted is adjusted such that each Tx for each case contributes 1000 molecules around the peak of the overall received signal.

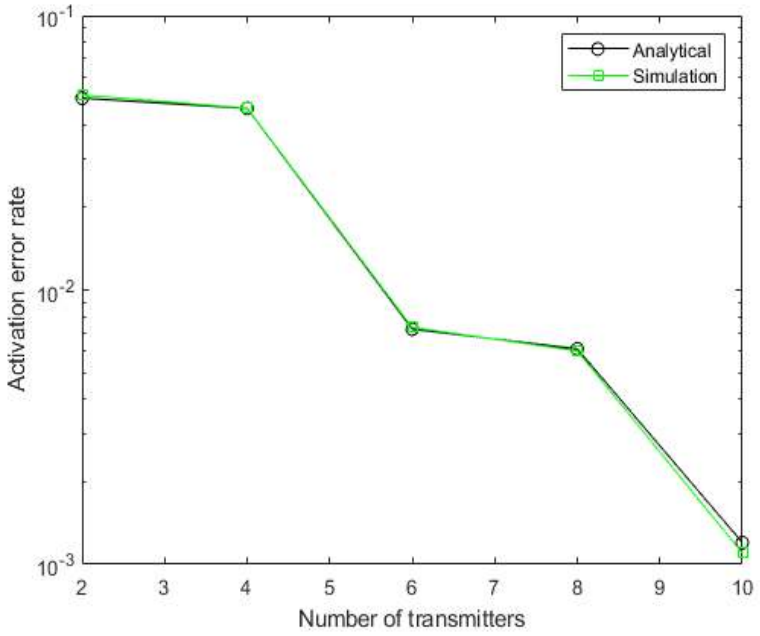

Figure 5.6: The analytical and simulation results for the predefined thresholding scenario of the ULA topology.

The threshold value for the topology with two Txs with the predefined thresholding scenario is selected as $\gamma = \frac{N_{Rx_1}[t_p-\frac{\tau}{2},t_p+\frac{\tau}{2}](1,0)+N_{Rx_1}[t_p-\frac{\tau}{2},t_p+\frac{\tau}{2}](0,0)}{2}$. The same idea is followed for $K>1$, where the first term in the threshold value represents the ideal case. In other words, the threshold values are $\gamma_K = 500, 1000, 1500, 2000, 2500$ for $K = 1, 2, 3, 4, 5$. As it can be seen from Figure 5.6, the computer simulation results fit the analytical ones almost perfectly. As expected, the activation error rate drops up to 10^{-3} for $K=5$. Moreover, an interesting behavior can be observed from these curves. The activation error rate drops following a staircase-like shape. The accuracy is observed to be higher for odd values of K, compared to even values. This can be explained by thinking the activation of a Rx as a decision done by the Txs, so, when K is odd, the result of their "majority vote" is more apparent.

The results for the mutual-thresholding case are provided in Figure 5.7. There is a clear improvement in the activation error rate, compared with the results presented earlier. This comes at the cost of assuming a communication channel between the Rxs such that they co-decide which one is to be activated. As a result, it can be

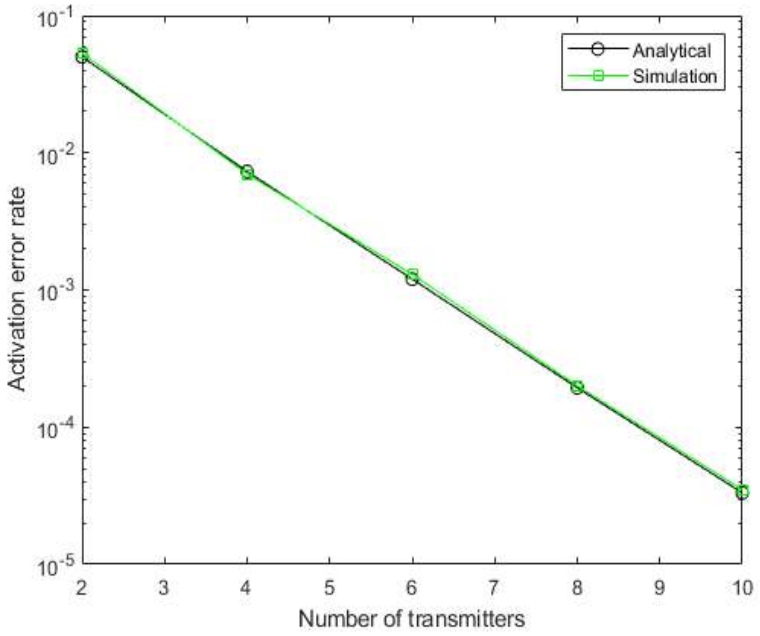

Figure 5.7: The analytical and simulation results for the mutual thresholding scenario of the ULA topology.

said that there exists a trade-off between the system's complexity and the overall achieved accuracy.

The threshold value for the composite error scenario is a key parameter, because a low value would reduce the activation error while causing the deactivation error to increase, and a high value would do the opposite. In order to minimize the overall error for this case, the analytical optimized γ is found by (17). The analytical results are then compared with simulation results, and the overall composite error rate curves are presented in Figure 5.8. The γ values used in the simulations are $\gamma_K = 490, 650, 1750, 1940, 2900$ for $K = 1, 2, 3, 4, 5$, respectively. One example of how the total composite error changes with respect to the threshold value is shown in Figure 5.10, where $\gamma = 650$ is selected among the values that provide the minimum actuation error rate. Similar behaviors are obtained for other K values as well.

Similar to the behavior of the curves in Figure 5.6, it can be concluded that an odd value of K ensures a better performance for the composite error case, as it enables the scheme to be less prone to the deactivation error. Another interesting

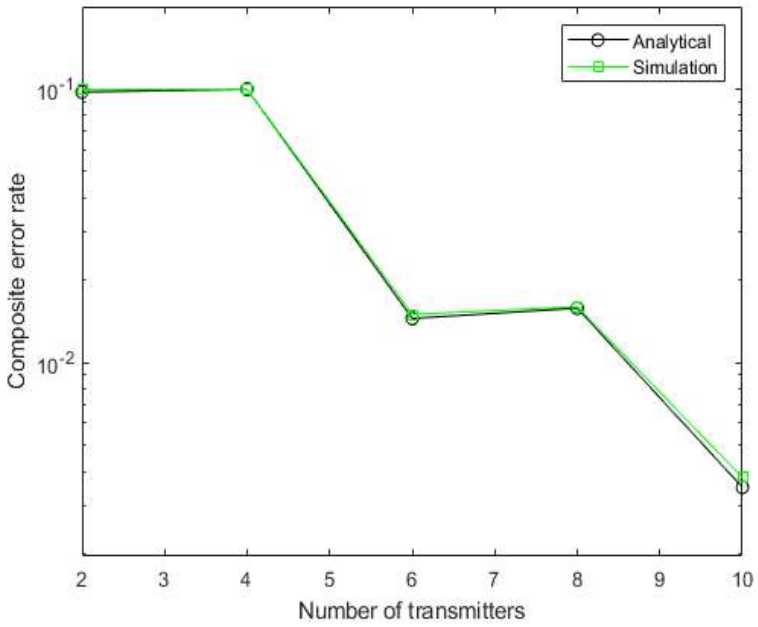

Figure 5.8: The analytical and simulation results for the composite error scenario of the ULA topology.

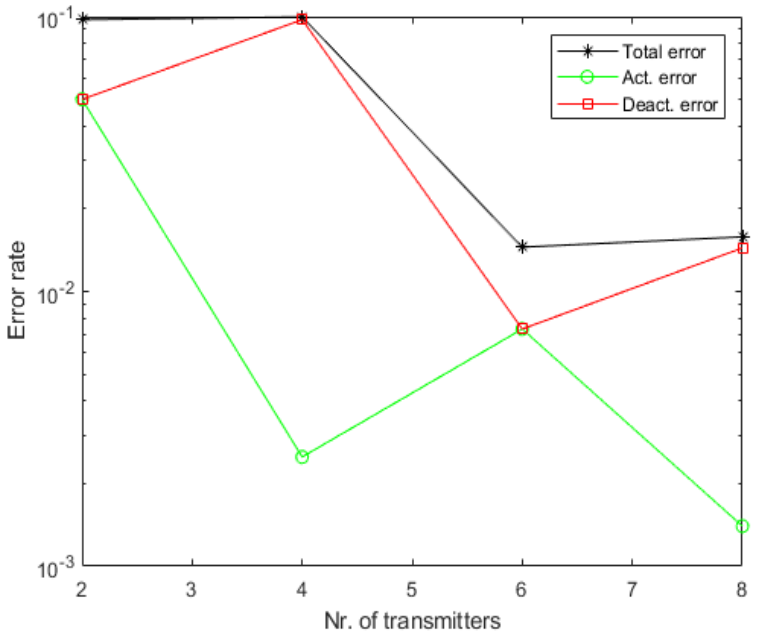

Figure 5.9: The activation and deactivation error components for the ULA topology.

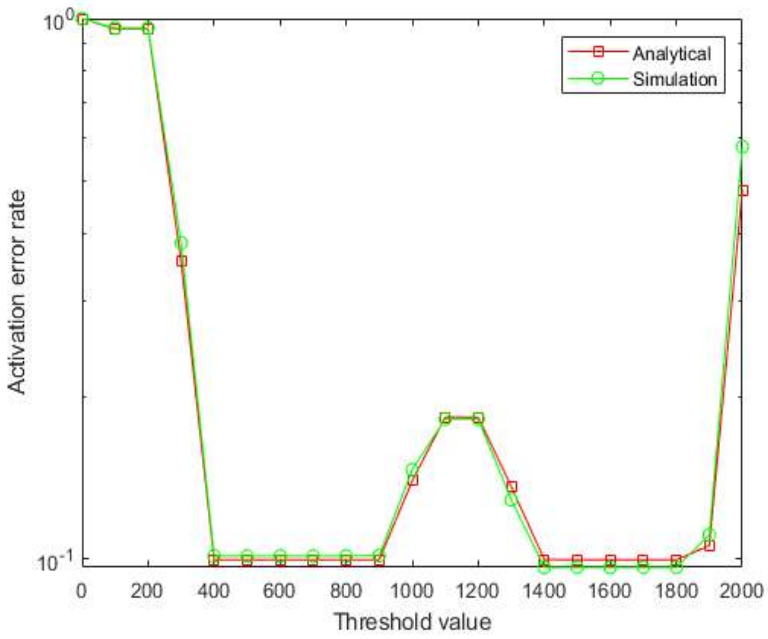

Figure 5.10: The composite error versus threshold value for the $K = 2$ ULA case.

result is obtained when the two error sources, namely, activation and deactivation errors are obtained separately. The results are presented in Figure 5.9. It can be concluded that for the composite error case, the deactivation error is dominating and the overall error is actually following its trend.

Lastly, the results of the composite error scenario for the random topology presented in the previous sections are provided. As it is shown in Figure 5.11, the performance of the random topology has similar characteristics with the ULA topology. The optimized γ values are $\gamma_K = 430, 780, 1940, 2825, 3760$ for $K = 1, 2, 3, 4, 5$, respectively.

It is noteworthy to mention that the case where all the power is allocated to the closest Tx to the intended Rx performs worse, since the accuracy actually increases when the sensors take the actuation decision altogether. Apart from that, even if all the sensors are used for an activation the performance is worse, since in that case, an error is more probable due to the possible emissions from the non-contributing sensors.

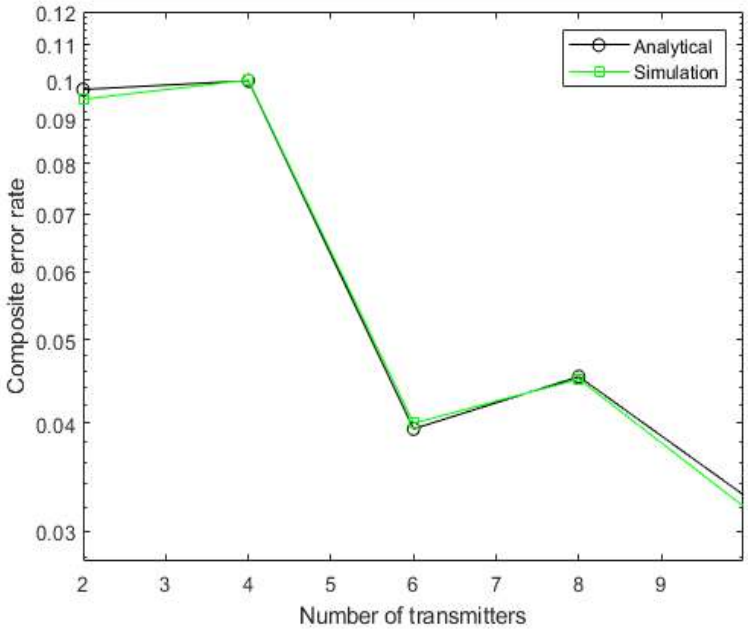

Figure 5.11: The analytical and simulation results for the composite error scenario of the random topology.

Chapter 6

CONCLUSION

To sum up, this dissertation has explored the MC literature and the main challenges faced by it. Two novel relay-based schemes have been proposed, addressing two different problems: the first one dealing with asymmetrical links of a two Txs one relay system, whereas the second one aims boosting the received signal shape by the assist of the relay node. Moreover, a molecular beamforming scheme for improving the actuation accuracy in MC networks has been. Apart from the purpose of these works to improve the overall performance of MC networks, coexistence of multiple nanomachines is required to make the MC's applications possible. For these reasons, the proposed schemes can find usage in different practical scenarios.

The first chapter of this dissertation has focused on providing the foundations of MC, its usage areas and the characteristics of the SISO topology. A brief introduction to the current literature on relaying in MC has been provided as well.

In the first contributing work, asymmetric communication links of the UL of a relay scheme have been investigated, for which error protection and communication fairness of these links have been improved by considering the proposed optimization solutions. Two solutions, which optimize the parameters of the further Tx's communication link, have been presented. The first one is based on optimizing its diffusion coefficient only given the other system parameters, whereas the other has taken into account both the diffusion coefficient and the number of emitted molecules. In order to compare the obtained results, channel coefficients, CDF, and BER curves have been provided. It is noted that the obtained solutions can be similarly extended to the DL of a relaying system, due to the channel symmetry. However, for simplicity purposes, only UL transmission has been considered in this work. Moreover, this idea could be further extended to a relay scheme with higher number of Txs as well as it could be incorporated to the IM technique for further improvement of the data

rate of the system.

The second contribution is a novel intelligent relaying MCvD scheme, which has been proposed in order to enhance the overall performance of the system. A relay has been placed between the Tx and the Rx pair with the purpose of collecting LoS molecules until time τ. Thus, the collected molecules are then emitted towards the Rx with some delay. The signal strength at the Rx side has been significantly boosted, improving the error rates considerably. The delay parameter is crucial, as it leads to a trade-off between signal improvement and ISI level. In order to find the best τ value, an optimization problem based on the SID function has been proposed. An analytical model for the intelligent relaying has been introduced, in order to optimize the SID function. Comparisons between the proposed model and simulation results have been drawn, as well as BER analysis for the proposed scheme. Lastly, the improvement in BER values as a result of this scheme has been observed.

The intelligent relaying scheme can be also introduced to more complex scenarios, such as MIMO setting. Additional future work might include amplification of the fraction of the molecules absorbed by the relay in order to further improve the overall performance. Optimization of other parameters, such as relay positioning might be jointly studied with τ optimization as well.

Lastly, a novel molecular beamforming design has been proposed in order to increase the actuation accuracy in MC networks. This design may find application on different tasks related to nano scale medicine and health care. The proposed system consists of several transmitting nodes, which, according to the application, aim to activate one Rx at a time. Given that there exists a probability of sensing error, it has been claimed that if the number of Txs is increased, the actuation accuracy is improved as well. The goal is to improve the quality of the signal received at the intended Rx, and to do so, there are several design characteristics followed throughout the study. First of all, given the node that has to be active, a Tx has to emit or stay quiet, based on whether its contribution to that node's received signal is constructive or not. Secondly, the Txs emit with a predefined delay time, such that the peaks of the received signal components almost overlap

at the Rx side. Moreover, since errors may occur, the number of emitted molecules has been adjusted beforehand, in order for each Tx to contribute the same towards the activation of the Rx node. This is because of the case in which the Tx which contributes the most stays quiet by mistake and the probability of an actuation error to occur is higher.

The proposed design has been validated both analytically and by means of computer simulations. Three different scenarios for computing the actuation error have been presented, and the analytical derivation has been provided for each. The ULA placement of Txs has been presented first for simplifying the concept of beamforming. A more realistic scenario has been presented as well. It has been concluded that there exists a trade-off between the actuation accuracy and system's complexity. Moreover, the system performs better when the number of Txs used to activate a Rx node is odd.

As this is a pioneering work on molecular beamforming, future works may focus on further optimizing this system and its parameters. Such optimization may include γ, τ and the contribution of molecules from each Tx around the peak. Moreover, further improvement may be done in regard to the computation of the signals' peak times, as in this study, they have been roughly estimated.

BIBLIOGRAPHY

[Abbasi et al., 2016] Abbasi, Q. H., Yang, K., Chopra, N., Jornet, J. M., Abuali, N. A., Qaraqe, K. A., and Alomainy, A. (2016). Nano-communication for biomedical applications: A review on the state-of-the-art from physical layers to novel networking concepts. *IEEE Access*, 4:3920–3935.

[Aberer et al., 2020] Aberer, F., Theiler-Schwetz, V., Ziko, H., Hausegger, B., Wiederstein-Grasser, I., Hochfellner, D. A., Eller, P., Tomberger, G., Ellmerer, M., Mader, J. K., et al. (2020). Accuracy and stability of an arterial sensor for glucose monitoring in a porcine model using glucose clamp technique. *Scientific Reports*, 10(1):1–9.

[Ahmadzadeh et al., 2015a] Ahmadzadeh, A., Noel, A., Burkovski, A., and Schober, R. (2015a). Amplify-and-forward relaying in two-hop diffusion-based molecular communication networks. In *2015 IEEE Global Communications Conference (GLOBECOM)*, pages 1–7. IEEE.

[Ahmadzadeh et al., 2015b] Ahmadzadeh, A., Noel, A., and Schober, R. (2015b). Analysis and design of multi-hop diffusion-based molecular communication networks. *IEEE Transactions on Molecular, Biological and Multi-Scale Communications*, 1(2):144–157.

[Akdeniz et al., 2018] Akdeniz, B. C., Turgut, N. A., Yilmaz, H. B., Chae, C.-B., Tugcu, T., and Pusane, A. E. (2018). Molecular signal modeling of a partially counting absorbing spherical receiver. *IEEE Transactions on Communications*, 66(12):6237–6246.

[Akyildiz et al., 2008] Akyildiz, I. F., Brunetti, F., and Blázquez, C. (2008). Nanonetworks: A new communication paradigm. *Computer Networks*, 52(12):2260–2279.

[Akyildiz et al., 2015] Akyildiz, I. F., Pierobon, M., Balasubramaniam, S., and Koucheryavy, Y. (2015). The internet of bio-nano things. *IEEE Communications Magazine*, 53(3):32–40.

[Alberts et al., 2003] Alberts, B., Johnson, A., Lewis, J., Raff, M., Roberts, K., Walter, P., et al. (2003). Molecular biology of the cell. *Scandinavian Journal of Rheumatology*, 32(2):125–125.

[Alomainy et al., 2019] Alomainy, A., Yang, K., Imran, M., Yao, X.-W., and Abbasi, Q. H. (2019). *Nano-Electromagnetic Communication at Terahertz and Optical Frequencies: Principles and Applications*. Institution of Engineering and Technology.

[Aloraefy et al., 2014] Aloraefy, M., Pfefer, T. J., Ramella-Roman, J. C., and Sapsford, K. E. (2014). In vitro evaluation of fluorescence glucose biosensor response. *Sensors*, 14(7):12127–12148.

[Alshammri et al., 2018] Alshammri, G. H., Ahmed, W. K., and Lawrence, V. B. (2018). Synchronous cooperative relaying technique for three-dimensional diffusion-based molecular nano communication networks. In *2018 IEEE 12th International Conference on Nano/Molecular Medicine and Engineering (NANOMED)*, pages 154–159. IEEE.

[Ardeshiri et al., 2017] Ardeshiri, G., Jamshidi, A. A., and Keshavarz-Haddad, A. (2017). Optimal relay location in diffusion based molecular communication. In *The 3rd Iranian Conference on Communications Engineering (ICCE 2017)*.

[Arjmandi et al., 2013] Arjmandi, H., Gohari, A., Kenari, M. N., and Bateni, F. (2013). Diffusion-based nanonetworking: A new modulation technique and performance analysis. *IEEE Communications Letters*, 17(4):645–648.

[Basar et al., 2019] Basar, E., Di Renzo, M., De Rosny, J., Debbah, M., Alouini, M.-S., and Zhang, R. (2019). Wireless communications through reconfigurable intelligent surfaces. *IEEE access*, 7:116753–116773.

[Cevallos et al., 2019] Cevallos, Y., Tello-Oquendo, L., Inca, D., Ghose, D., Shirazi, A. Z., and Gomez, G. A. (2019). Health applications based on molecular communications: a brief review. In *2019 IEEE International Conference on E-health Networking, Application & Services (HealthCom)*, pages 1–6. IEEE.

[Chahibi, 2017] Chahibi, Y. (2017). Molecular communication for drug delivery systems: A survey. *Nano Communication Networks*, 11:90–102.

[Chahibi et al., 2013] Chahibi, Y., Pierobon, M., Song, S. O., and Akyildiz, I. F. (2013). A molecular communication system model for particulate drug delivery systems. *IEEE Transactions on biomedical engineering*, 60(12):3468–3483.

[Chouhan and Sharma, 2020] Chouhan, L. and Sharma, P. K. (2020). Molecular communication in three-dimensional diffusive channel with mobile nanomachines. *Nano Communication Networks*, 24:100296.

[Chude-Okonkwo et al., 2019] Chude-Okonkwo, U., Malekian, R., and Maharaj, B. (2019). *Advanced Targeted Nanomedicine*. Springer.

[Deng et al., 2016] Deng, Y., Guo, W., Noel, A., Nallanathan, A., and Elkashlan, M. (2016). Enabling energy efficient molecular communication via molecule energy transfer. *IEEE Communications Letters*, 21(2):254–257.

[Dennis Jr and Schnabel, 1996] Dennis Jr, J. E. and Schnabel, R. B. (1996). *Numerical methods for unconstrained optimization and nonlinear equations*. SIAM.

[DiSanto et al., 2015] DiSanto, R. M., Subramanian, V., and Gu, Z. (2015). Recent advances in nanotechnology for diabetes treatment. *Wiley Interdisciplinary Reviews: Nanomedicine and Nanobiotechnology*, 7(4):548–564.

[Dürr et al., 1981] Dürr, D., Goldstein, S., and Lebowitz, J. (1981). A mechanical model of brownian motion. *Communications in Mathematical Physics*, 78(4):507–530.

[Einolghozati et al., 2013] Einolghozati, A., Sardari, M., and Fekri, F. (2013). Relaying in diffusion-based molecular communication. In *2013 IEEE International Symposium on Information Theory*, pages 1844–1848. IEEE.

[El-Hajj and Chahine, 2021] El-Hajj, A. M. and Chahine, K. (2021). In-vivo automated diabetes control system utilizing molecular communication. In *2021 4th International Conference on Bio-Engineering for Smart Technologies (BioSMART)*, pages 1–4. IEEE.

[Felicetti et al., 2014] Felicetti, L., Femminella, M., Reali, G., and Liò, P. (2014). Endovascular mobile sensor network for detecting circulating tumoral cells. In *Proceedings of the 9th International Conference on Body Area Networks*, pages 111–117.

[Felicetti et al., 2016] Felicetti, L., Femminella, M., Reali, G., and Liò, P. (2016). Applications of molecular communications to medicine: A survey. *Nano Communication Networks*, 7:27–45.

[Fonseca et al., 2007] Fonseca, L., Cane, C., and Mazzolai, B. (2007). Application of micro and nanotechnologies to food safety and quality monitoring. *Measurement and Control*, 40(4):116–119.

[for Standardization, 2003] for Standardization, I. O. (2003). *In vitro diagnostic test systems: requirements for blood-glucose monitoring systems for self-testing in managing diabetes mellitus*. ISO.

[Galal and Hesselbach, 2018] Galal, A. and Hesselbach, X. (2018). Nano-networks communication architecture: Modeling and functions. *Nano Communication Networks*, 17:45–62.

[Ghazani et al., 2016] Ghazani, M. F., Aminian, G., Mirmohseni, M., Gohari, A., and Kenari, M. N. (2016). Physical layer network coding in molecular two-way relay networks. In *2016 Iran Workshop on Communication and Information Theory (IWCIT)*, pages 1–6. IEEE.

[Giné and Akyildiz, 2009] Giné, L. P. and Akyildiz, I. F. (2009). Molecular communication options for long range nanonetworks. *Computer Networks*, 53(16):2753–2766.

[Guo et al., 2015] Guo, W., Mias, C., Farsad, N., and Wu, J.-L. (2015). Molecular versus electromagnetic wave propagation loss in macro-scale environments. *IEEE Transactions on Molecular, Biological and Multi-Scale Communications*, 1(1):18–25.

[Gürsoy et al., 2017] Gürsoy, M. C., Akdeniz, B. C., Pusane, A. E., and Tuğcu, T. (2017). On the effects of mobile transmitter and receiver on the performance of molecular communications system. In *2017 25th Signal Processing and Communications Applications Conference (SIU)*, pages 1–4. IEEE.

[Gursoy et al., 2019a] Gursoy, M. C., Basar, E., Pusane, A. E., and Tugcu, T. (2019a). An ili mitigating modulation scheme for molecular mimo communications. In *2019 42nd International Conference on Telecommunications and Signal Processing (TSP)*, pages 28–31. IEEE.

[Gursoy et al., 2019b] Gursoy, M. C., Basar, E., Pusane, A. E., and Tugcu, T. (2019b). Index modulation for molecular communication via diffusion systems. *IEEE Transactions on Communications*, 67(5):3337–3350.

[Gursoy et al., 2020] Gursoy, M. C., Celik, A., Basar, E., Pusane, A. E., and Tugcu, T. (2020). Molecular index modulation with space-time equalization. *IEEE Wireless Communications Letters*, 9(5):702–705.

[Han et al., 2008] Han, J., Fu, J., and Schoch, R. B. (2008). Molecular sieving using nanofilters: past, present and future. *Lab on a Chip*, 8(1):23–33.

[Heren et al., 2015] Heren, A. C., Yilmaz, H. B., Chae, C.-B., and Tugcu, T. (2015). Effect of degradation in molecular communication: Impairment or enhancement? *IEEE Transactions on Molecular, Biological and Multi-Scale Communications*, 1(2):217–229.

[Hiyama et al., 2006] Hiyama, S., Moritani, Y., Suda, T., Egashira, R., Enomoto, A., Moore, M., and Nakano, T. (2006). Molecular communication. *Journal-Institute of Electronics Information and Communication Engineers*, 89(2):162.

[Jamshidi et al., 2019] Jamshidi, A., Keshavarz-Haddad, A., and Ardeshiri, G. (2019). Map detector performance analysis in diffusion-based relaying molecular communications. *Nano Communication Networks*, 19:81–91.

[Kadloor et al., 2012] Kadloor, S., Adve, R. S., and Eckford, A. W. (2012). Molecular communication using brownian motion with drift. *IEEE Transactions on NanoBioscience*, 11(2):89–99.

[Kara et al., 2021] Kara, O., Yaylali, G., Pusane, A. E., and Tugcu, T. (2021). Machine learning based molecular index modulation. *arXiv preprint arXiv:2103.09812*.

[Khaloopour et al., 2020] Khaloopour, L., Mirmohseni, M., and Nasiri-Kenari, M. (2020). Cooperative abnormality detection in fluidic medium molecular communication. In *2020 Iran Workshop on Communication and Information Theory (IWCIT)*, pages 1–6. IEEE.

[Khaloopour et al., 2021] Khaloopour, L., Mirmohseni, M., and Nasiri-Kenari, M. (2021). Theoretical concept study of cooperative abnormality detection and localization in fluidic-medium molecular communication. *IEEE Sensors Journal*, 21(15):17118–17130.

[Kilinc and Akan, 2013] Kilinc, D. and Akan, O. B. (2013). Receiver design for molecular communication. *IEEE Journal on Selected Areas in Communications*, 31(12):705–714.

[Kislal et al., 2020] Kislal, A. O., Akdeniz, B. C., Lee, C., Pusane, A. E., Tugcu, T., and Chae, C.-B. (2020). Isi-mitigating channel codes for molecular communication via diffusion. *IEEE Access*, 8:24588–24599.

[Koo et al., 2016] Koo, B.-H., Lee, C., Yilmaz, H. B., Farsad, N., Eckford, A., and Chae, C.-B. (2016). Molecular mimo: From theory to prototype. *IEEE Journal on Selected Areas in Communications*, 34(3):600–614.

[Kuran et al., 2020] Kuran, M. Ş., Yilmaz, H. B., Demirkol, I., Farsad, N., and Goldsmith, A. (2020). A survey on modulation techniques in molecular communication via diffusion. *IEEE Communications Surveys & Tutorials*, 23(1):7–28.

[Kuscu et al., 2019] Kuscu, M., Dinc, E., Bilgin, B. A., Ramezani, H., and Akan, O. B. (2019). Transmitter and receiver architectures for molecular communications: A survey on physical design with modulation, coding, and detection techniques. *Proceedings of the IEEE*, 107(7):1302–1341.

[Llatser et al., 2011] Llatser, I., Alarcón, E., and Pierobony, M. (2011). Diffusion-based channel characterization in molecular nanonetworks. In *2011 IEEE Conference on Computer Communications Workshops (INFOCOM WKSHPS)*, pages 467–472. IEEE.

[Mahfuz et al., 2010] Mahfuz, M. U., Makrakis, D., and Mouftah, H. T. (2010). On the characterization of binary concentration-encoded molecular communication in nanonetworks. *Nano Communication Networks*, 1(4):289–300.

[Mosayebi et al., 2018] Mosayebi, R., Wicke, W., Jamali, V., Ahmadzadeh, A., Schober, R., and Nasiri-Kenari, M. (2018). Advanced target detection via molecular communication. In *2018 IEEE Global Communications Conference (GLOBECOM)*, pages 1–7. IEEE.

[Murin et al., 2017] Murin, Y., Farsad, N., Chowdhury, M., and Goldsmith, A. (2017). Time-slotted transmission over molecular timing channels. *Nano communication networks*, 12:12–24.

[Nakano and Shuai, 2011] Nakano, T. and Shuai, J. (2011). Repeater design and modeling for molecular communication networks. In *2011 IEEE conference on*

computer communications workshops (INFOCOM WKSHPS), pages 501–506. IEEE.

[Pierobon and Akyildiz, 2010] Pierobon, M. and Akyildiz, I. F. (2010). A physical end-to-end model for molecular communication in nanonetworks. *IEEE Journal on Selected Areas in Communications*, 28(4):602–611.

[Shi and Yang, 2017] Shi, L. and Yang, L.-L. (2017). Error performance analysis of diffusive molecular communication systems with on-off keying modulation. *IEEE Transactions on Molecular, Biological and Multi-Scale Communications*, 3(4):224–238.

[Shitharth et al., 2021] Shitharth, S., Meshram, P., Kshirsagar, P. R., Manoharan, H., Tirth, V., and Sundramurthy, V. P. (2021). Impact of big data analysis on nanosensors for applied sciences using neural networks. *Journal of Nanomaterials*, 2021.

[Tavakkoli et al., 2017] Tavakkoli, N., Azmi, P., and Mokari, N. (2017). Optimal positioning of relay node in cooperative molecular communication networks. *IEEE Transactions on Communications*, 65(12):5293–5304.

[Tepekule et al., 2015a] Tepekule, B., Pusane, A. E., Kuran, M. Ş., and Tugcu, T. (2015a). A novel pre-equalization method for molecular communication via diffusion in nanonetworks. *IEEE Communications letters*, 19(8):1311–1314.

[Tepekule et al., 2015b] Tepekule, B., Pusane, A. E., Yilmaz, H. B., Chae, C.-B., and Tugcu, T. (2015b). Isi mitigation techniques in molecular communication. *IEEE Transactions on Molecular, Biological and Multi-Scale Communications*, 1(2):202–216.

[Tiwari and Upadhyay, 2017] Tiwari, S. K. and Upadhyay, P. K. (2017). Estimate-and-forward relaying in diffusion-based molecular communication networks: Performance evaluation and threshold optimization. *IEEE Transactions on Molecular, Biological and Multi-Scale Communications*, 3(3):183–193.

[Van Veen and Buckley, 1988] Van Veen, B. D. and Buckley, K. M. (1988). Beamforming: A versatile approach to spatial filtering. *IEEE assp magazine*, 5(2):4–24.

[Varshney et al., 2018a] Varshney, N., Jagannatham, A. K., and Varshney, P. K. (2018a). On diffusive molecular communication with mobile nanomachines. In *2018 52nd Annual Conference on Information Sciences and Systems (CISS)*, pages 1–6. IEEE.

[Varshney et al., 2018b] Varshney, N., Patel, A., Deng, Y., Haselmayr, W., Varshney, P. K., and Nallanathan, A. (2018b). Abnormality detection inside blood vessels with mobile nanomachines. *IEEE Transactions on Molecular, Biological and Multi-Scale Communications*, 4(3):189–194.

[Wang et al., 2021] Wang, J., Peng, M., and Liu, Y. (2021). Performance analysis of diffusion-based decode-and-forward relay with depleted molecule shift keying. *Digital Communications and Networks*, 7(3):399–409.

[Wang et al., 2019] Wang, J., Peng, M., Liu, Y., Liu, X., and Daneshmand, M. (2019). Performance analysis of signal detection for amplify-and-forward relay in diffusion-based molecular communication systems. *IEEE Internet of Things Journal*, 7(2):1401–1412.

[Wang et al., 2017] Wang, J., Yuan, S., and Peng, M. (2017). Performance analysis and optimal signal detection for amplify-and-forward relay in diffusion-based molecular communication systems. In *2017 IEEE/CIC International Conference on Communications in China (ICCC)*, pages 1–6. IEEE.

[Wang et al., 2015] Wang, X., Higgins, M. D., and Leeson, M. S. (2015). Relay analysis in molecular communications with time-dependent concentration. *IEEE Communications Letters*, 19(11):1977–1980.

[Wu et al., 2020] Wu, C., Lin, L., Guo, W., and Yan, H. (2020). Signal detection for molecular mimo communications with asymmetrical topology. *IEEE Transactions on Molecular, Biological and Multi-Scale Communications*, 6(1):60–70.

[Yang et al., 2019] Yang, L., Ge, X., Liu, Q., Yang, K., Chen, Y., and Nakano, T. (2019). Chemotaxis-based multi-hop molecular nanonetworks for target detection. In *2019 IEEE/CIC International Conference on Communications Workshops in China (ICCC Workshops)*, pages 186–191. IEEE.

[Yaylali et al., 2021] Yaylali, G., Akdeniz, B. C., Tugcu, T., and Pusane, A. E. (2021). Channel modeling for multi-receiver molecular communication systems. *arXiv preprint arXiv:2111.09302*.

[Yilmaz and Chae, 2014a] Yilmaz, H. B. and Chae, C.-B. (2014a). Arrival modelling for molecular communication via diffusion. *Electronics Letters*, 50(23):1667–1669.

[Yilmaz and Chae, 2014b] Yilmaz, H. B. and Chae, C.-B. (2014b). Simulation study of molecular communication systems with an absorbing receiver: Modulation and isi mitigation techniques. *Simulation Modelling Practice and Theory*, 49:136–150.

[Yilmaz et al., 2015] Yilmaz, H. B., Chae, C.-B., Tepekule, B., and Pusane, A. E. (2015). Arrival modeling and error analysis for molecular communication via diffusion with drift. In *Proceedings of the Second Annual International Conference on Nanoscale Computing and Communication*, pages 1–6.

[Yilmaz et al., 2014] Yilmaz, H. B., Heren, A. C., Tugcu, T., and Chae, C.-B. (2014). Three-dimensional channel characteristics for molecular communications with an absorbing receiver. *IEEE Communications Letters*, 18(6):929–932.

[Yin et al., 2017] Yin, B., Ji, X., and Peng, M. (2017). Performance analysis for cooperative relaying in diffusion-based molecular communication. In *2017 9th International Conference on Wireless Communications and Signal Processing (WCSP)*, pages 1–6. IEEE.

[Young et al., 1996] Young, H. D., Freedman, R. A., Sandin, T., and Ford, A. L. (1996). *University physics*, volume 9. Addison-Wesley Reading, MA.

[Yuan et al., 2018] Yuan, S., Wang, J., and Peng, M. (2018). Performance analysis of reversible binding receptor based decode-and-forward relay in molecular communication systems. *IEEE Wireless Communications Letters*, 7(5):880–883.